Variations in microbial carbon sources and cycling in the deep continental subsurface

ARTICLE *in* GEOCHIMICA ET COSMOCHIMICA ACTA · OCTOBER 2015

Impact Factor: 4.33 · DOI: 10.1016/j.gca.2015.10.003

Available online at www.sciencedirect.com

ScienceDirect

Geochimica et Cosmochimica Acta 173 (2016) 264–283

Geochimica et Cosmochimica Acta

www.elsevier.com/locate/gca

Variations in microbial carbon sources and cycling in the deep continental subsurface

Danielle N. Simkus [a], Greg F. Slater [a,*], Barbara Sherwood Lollar [b], Kenna Wilkie [b], Thomas L. Kieft [c], Cara Magnabosco [d], Maggie C.Y. Lau [d], Michael J. Pullin [e], Sarah B. Hendrickson [e], K. Eric Wommack [f], Eric G. Sakowski [f], Esta van Heerden [g], Olukayode Kuloyo [g], Borja Linage [g], Gaetan Borgonie [g,1], Tullis C. Onstott [d]

[a] *School of Geography and Earth Sciences, McMaster University, Hamilton, Ontario, Canada*
[b] *Department of Earth Sciences, University of Toronto, Toronto, Ontario, Canada*
[c] *Department of Biology, New Mexico Institute of Mining and Technology, Socorro, NM, USA*
[d] *Department of Geosciences, Princeton University, Princeton, NJ, USA*
[e] *Department of Chemistry, New Mexico Institute of Mining and Technology, Socorro, NM, USA*
[f] *Department of Plant and Soil Sciences, Delaware Biotechnology Institute, Newark, DE, USA*
[g] *Department of Microbial, Biochemical and Food Biotechnology, University of the Free State, Bloemfontein, South Africa*

Received 11 December 2014; accepted in revised form 6 October 2015; Available online 19 October 2015

Abstract

Deep continental subsurface fracture water systems, ranging from 1.1 to 3.3 km below land surface (kmbls), were investigated to characterize the indigenous microorganisms and elucidate microbial carbon sources and their cycling. Analysis of phospholipid fatty acid (PLFA) abundances and direct cell counts detected varying biomass that was not correlated with depth. Compound-specific carbon isotope analyses ($\delta^{13}C$ and $\Delta^{14}C$) of the phospholipid fatty acids (PLFAs) and carbon substrates combined with genomic analyses did identify, however, distinct carbon sources and cycles between the two depth ranges studied.

In the shallower boreholes at circa 1 kmbls, isotopic evidence indicated microbial incorporation of biogenic CH_4 by the *in situ* microbial community. At the shallowest site, 1.05 kmbls in Driefontein mine, this process clearly dominated the isotopic signal. At slightly deeper depths, 1.34 kmbls in Beatrix mine, the isotopic data indicated the incorporation of both biogenic CH_4 and dissolved inorganic carbon (DIC) derived from CH_4 oxidation. In both of these cases, molecular genetic analysis indicated that methanogenic and methanotrophic organisms together comprised a small component (<5%) of the microbial community. Thus, it appears that a relatively minor component of the prokaryotic community is supporting a much larger overall bacterial community in these samples.

In the samples collected from >3 kmbls in Tau Tona mine (TT107, TT109 Bh2), the CH_4 had an isotopic signature suggesting a predominantly abiogenic origin with minor inputs from microbial methanogenesis. In these samples, the isotopic enrichments ($\delta^{13}C$ and $\Delta^{14}C$) of the PLFAs relative to CH_4 were consistent with little incorporation of CH_4 into the biomass. The most ^{13}C-enriched PLFAs were observed in TT107 where the dominant CO_2-fixation pathway was the acetyl-CoA

* Corresponding author at: School of Geography and Earth Sciences, Room 306, General Sciences Building, McMaster University, Hamilton, Ontario L8S 4L8, Canada. Tel.: +1 (905) 525 9140x26388; fax: +1 (905) 546 0463.
[1] Current address: Extreme Life Isyensya, PB 65, 9050 Gentbrugge, Belgium.

http://dx.doi.org/10.1016/j.gca.2015.10.003

pathway by non-acetogenic bacteria. The differences in the $\delta^{13}C$ of the PLFAs and the DIC and DOC for TT109 Bh2 were ~−24‰ and 0‰, respectively. The dominant CO_2-fixation pathways were 3-HP/4-HB cycle > acetyl-CoA pathway > reductive pentose phosphate cycle.

1. INTRODUCTION

The carbon sources and carbon cycling processes utilized by the Earth's deep continental subsurface biosphere are still poorly understood, despite the global significance of these microbial systems (Onstott et al., 1998; Whitman et al., 1998; Pfiffner et al., 2006). Constraining these processes is an integral step in defining the limits of habitability on Earth, while providing insight into the potential for life to exist in the deep subsurface of other planetary bodies. Although photosynthetically derived organic carbon buried within Earth's subsurface can be utilized as a carbon source by subsurface microbial communities, this organic carbon source is limiting in many deep terrestrial subsurface environments (Pedersen, 2000). In systems where complex organic carbon is limited, microbial communities must rely on either autotrophic fixation of dissolved inorganic carbon (DIC) by chemolithoautotrophs, including methanogens, acetogens, sulphate reducers and iron reducers (Chivian et al., 2008; Beal et al., 2009; Lau et al., 2014; Stevens and McKinley, 1995; Pedersen, 2000; Sherwood Lollar et al., 2006; Magnabosco et al., 2015) or oxidation of CH_4 by methanotrophs (Bowman et al., 1993; Kotelnikova, 2002; Mills et al., 2010).

Energy sources for chemolithoautotrophic communities (e.g. H_2) can be produced via several abiotic processes, including magmatic gas reactions, cataclasis of silicates, hydrolysis of ferrous minerals, the gas shift reaction and radiolytic decomposition of water (Apps and van de Kamp, 1993; Pedersen, 1997; Lin et al., 2005; Etiope and Sherwood Lollar, 2013; Stevens and McKinley, 1995). Methanogens and acetogens couple DIC reduction to H_2 oxidation to produce CH_4 and acetate, respectively. Alternatively, abiogenic hydrocarbon production via Fischer–Tropsch-type synthesis reactions, whereby CO/CO_2 and H_2 react to produce hydrocarbons of various molecular weights including CH_4 (Sherwood Lollar et al., 2002), can provide CH_4 and higher hydrocarbons as potential carbon substrates for methanotrophs and heterotrophs to support subsurface microbial communities independent of photosynthetically-derived organic matter.

Microbial oxidation of CH_4 is carried out by both aerobic bacteria that utilize CH_4 monooxygenase (MMO; Bowman, 2006) and anaerobic archaea that utilize portions of the autotrophic methanogenesis pathway in reverse (Knittel and Boetius, 2009) and work in consortia with bacteria, such as sulphate reducers (Hoehler et al., 1994; Hinrichs et al., 1999; Boetius et al., 2000). Recently the ANME-2 clade of archaea has been shown to perform anaerobic oxidation of CH_4 (AOM), by coupling CH_4 oxidation to sulphate reduction (Milucka et al., 2012) or nitrate reduction (Haroon et al., 2013) within the same microorganism. Oxidation of CH_4 under anaerobic conditions by bacteria has also been shown to occur by the denitrifying *Candidatus* "Methylomirabilis oxyfera", which produces intracellular O_2 by dismutation of NO (Ettwig et al., 2010, 2012). Although aerobic CH_4 oxidation has been reported in terrestrial deep subsurface habitats (Bowman et al., 1993; Kotelnikova, 2002; Mills et al., 2010), the occurrence of anaerobic CH_4 oxidation in this setting has not yet been reported in the literature.

Comparison of the natural abundances of ^{13}C and ^{14}C in membrane phospholipid fatty acids (PLFAs) and in potential carbon sources can elucidate microbial carbon sources (Petsch et al., 2001; Slater et al., 2005). Further, such comparison can identify the putative pathways being used to assimilate carbon and, in some cases, deduce the *in situ* metabolic rates. The $\delta^{13}C$ value of microbial PLFAs depends on the following: (1) the $\delta^{13}C$ value of the source of the assimilated carbon; (2) kinetic isotope effects (KIEs) associated with the carbon assimilation pathway (e.g. autotrophy vs. heterotrophy vs. CH_4 oxidation); and (3) KIEs involved in the microbial synthesis of PLFAs (Hayes, 2001; Boschker and Middelburg, 2002). Carbon fixation pathways involved in autotrophic metabolisms generally produce organic components, and particularly PLFAs, that are depleted in ^{13}C relative to the DIC source, but the extent of this carbon isotope fractionation is highly variable (Boschker and Middelburg, 2002; Berg et al., 2010). For example, autotrophic sulphate-reducing bacteria have been found to produce PLFAs that are up to 58‰ more depleted in ^{13}C than DIC (Londry et al., 2004); whereas other autotrophic bacteria produce PLFAs that are only several ‰ more depleted than DIC (Boschker and Middelburg, 2002). For heterotrophic metabolisms, PLFAs produced in aerobic environments generally show relatively small carbon isotope fractionations, producing $\delta^{13}C_{PLFA}$ values that are typically 4–8‰ more depleted than the dissolved organic carbon (DOC) source. However, in anaerobic environments, heterotrophic bacteria have been shown to produce PLFAs that are up to 21‰ more depleted than their DOC substrate (Teece et al., 1999; Boschker and Middelburg, 2002); and sulphate-reducing bacteria produce PLFAs that are 9.5‰ more enriched when oxidizing acetate (Londry et al., 2004). Lastly, microbial aerobic oxidation of CH_4 generally results in particularly depleted $\delta^{13}C_{PLFA}$ values because $\delta^{13}C_{CH4}$ values are typically very negative and carbon isotope fractionations ($\Delta^{13}C_{CH4\text{-}PLFA}$) can range from 2‰ to 30‰ less enriched than the CH_4 substrate, depending on the carbon fixation pathways (RuMP for Type I and X methanotrophs and Serine pathway for Type II methanotrophs) and experimental conditions (Jahnke et al., 1999; Whiticar, 1999; Valentine and Reeburgh, 2000; Templeton et al., 2006).

Because the variability in the fractionations of stable carbon isotopes can obfuscate a definitive identification of the carbon substrate, radiocarbon ($\Delta^{14}C$) analyses of PLFAs and potential carbon substrates have been successfully used to differentiate microbial carbon sources (Petsch et al., 2001; Slater et al., 2005, 2006; Brady et al., 2009; Mills et al., 2010, 2013; Seifert et al., 2013). As $\Delta^{14}C$ values are normalized to a $\delta^{13}C_{PLFA}$ of −25‰, the effects of any KIEs involved in biosynthesis are removed (Stuiver and Polach, 1977), and the $\Delta^{14}C$ values can be directly compared to that of potential carbon sources and metabolic products (Slater et al., 2005).

In this study, we compared the $\delta^{13}C$ and $\Delta^{14}C$ of PLFAs of planktonic microbial communities with that of their potential microbial carbon sources (DIC, DOC and CH_4) collected from six boreholes intersecting natural water-bearing fractures located in the deep mines of South Africa (1 to >3 kmbls). We combined these data with the relative abundances of key functional genes for CH_4 and CO_2 cycling pathways obtained from metagenomic analyses, and the microbial community composition derived from 16S rRNA gene analyses. This integrated database was used to determine the carbon sources, carbon assimilation pathways and carbon cycling rates of deep subsurface microbial communities.

2. MATERIALS AND METHODS

2.1. Study sites

The geology of the region has been previously described by Lin et al. (2005) and Onstott et al. (2006). In brief, the Witwatersrand Basin of South Africa is a large Archean, intracratonic basin composed of the 2.9 Ga Witwatersrand Supergroup (quartzite and minor Kimberley Group shale), overlain by the 2.7 Ga Ventersdorp Supergroup (mafic volcanic sequence), and the 2.45 Ga Transvaal Supergroup (dolomite, banded iron formation and volcanic units). Strata in the eastern and southern portions of the Witwatersrand Basin are overlain by the Permo-Carboniferous Karoo sandstone and shale. Six borehole samples from four mines in South Africa, Driefontein (DR), Beatrix (BE), Tau Tona (TT) and Kloof (KL), represent different geographical locations, depths and geological and geochemical settings.

Beatrix gold mine (Sibanye Gold Ltd.) is located approximately 240 km southwest of Johannesburg along the southwestern rim of the Witwatersrand Basin. The two sub-horizontal boreholes (BE326 Bh1 and BE326 Bh2) are located on level 26, <1 km south of the #3 shaft at a depth of 1.34 km below land surface (kmbls). They are located in the Witwatersrand Supergroup, which, at this location, is directly overlain by 200 m of Ventersdorp Supergroup metavolcanics, on top of which lies 500 m of the Carboniferous Karoo sediments (Lin et al. 2006). BE326 Bh2 penetrates 57 m into a medium- to coarse-grained, sub-lithic arenite before intersecting a NNW striking, pre-Karoo, fluid-filled fault. BE326 Bh1 penetrates ~50 m into the same quartzite unit before intersecting fracture fluid at the margins of a NW striking, Ventersdorp Supergroup dike. This dike is offset by the above fault very close to the position where BE326 Bh2 intersects it. The borehole fracture fluids are separated by ~50 m. Since they were first drilled in 2007, they have been sealed with high-pressure steel valves. The borehole BE326 Bh2 was sampled for PLFA and carbon isotope analyses in two successive years (2011 and 2012), allowing temporal variations to be assessed.

Driefontein gold mine (Sibanye Gold Ltd.) is situated 70 km west of Johannesburg on the northwestern rim of the Witwatersrand Basin. The sub-horizontal borehole (DR5IPC) was located at #5 shaft in the intermediate pumping chamber (IPC) at a depth of 1.05 kmbls and intersects the regional Malmani Subgroup dolomite aquifer, which occurs in the Transvaal Supergroup. This was an old borehole designed to tap the aquifer water for mine use, but was never employed as #5 shaft was never brought into production. At this location, the dolomite is completely overlain by banded iron formation and thus represents a confined aquifer where water flow occurs primarily through fractures in the dolomite.

Tau Tona gold mine (AngloGold Ashanti Co.) is located 3.8 km west of the DR5IPC borehole. The two sampling sites (TT107 and TT109 Bh2) were sub-horizontal boreholes located on levels 107 and 109 at depths of 3.05 and 3.14 kmbls, respectively. TT107 penetrated 400 m into medium-grained quartzite, crossing the 100-m wide Pretorius Fault Zone (Heesakkers et al., 2011) and intersecting the border of the NNE striking Jean's Dyke. TT109 Bh2 penetrated 100 m into medium-grained quartzite and also intersected the border of Jean's Dyke. Jean's Dyke is likely Karoo in age and cuts across all of the Precambrian strata. The water intersections of TT107 and TT109 Bh2 are separated by ~100 m horizontally and ~100 m vertically. Both of these boreholes were sealed off after intersecting water with high-pressure steel valves several weeks prior to collecting the samples.

Kloof gold mine (Sibanye Gold Ltd.) #4 shaft is located 12 km east of Driefontein #5 shaft. The sub-horizontal borehole sampled (KL445) was located on level 45 at a depth of 3.28 kmbls. The borehole penetrated metavolcanic units of the 2.7 Ga Ventersdorp Supergroup for <100 m before intersecting a fluid-filled fracture associated with Danie's fault, which is an EW striking normal fault that offsets units of the Ventersdorp Supergroup, but does not cut the overlying Transvaal Supergroup (Manzi et al., 2012).

The boreholes sampled at Beatrix and Driefontein gold mines are the same as those previously reported by Borgonie et al. (2011), from which nematodes were isolated.

2.2. Sampling methods

At each site, a sterile stainless steel manifold with 5 stainless steel valves, which had been previously combusted at 400 °C for 8 h and autoclaved, was connected to the borehole casing as a means of excluding mine air and other contaminants. The main valve and four side valves were opened to let the fracture water that was under natural high pressure flow for several minutes. This process flushed out any water that might have been oxygenated during the initial contact with mine air, and also

flushed air out of the sterile manifold. Autoclaved sampling tubes that were subsequently connected to the manifold were also flushed in a similar manner immediately after installation.

All water and gas samples were collected from the manifold tubing after the methods of Sherwood Lollar et al. (2002), Ward et al. (2004), Onstott et al. (2006) and Borgonie et al. (2011). Temperature, pH, conductivity and reduction potential (Eh) were measured from the water with hand-held probes (Hanna Instruments, Woonsocket, RI, USA, or Extech Instruments, Nashua, NH, USA), and dissolved O_2, H_2O_2, Fe(II), total Fe and sulfide were measured using Chemetrics test kits (Chemetrics Inc., Calverton, VA). Water for $\delta^{13}C_{DIC}$ analysis was filtered through a 0.2-μm filter into 40-mL glass amber vials, which were previously rinsed in 10% HCl, combusted at 450 °C for 8 h, and treated with 50 μL of saturated $HgCl_2$ solution prior to sampling. Water for $\Delta^{14}C_{DIC}$ analysis was filtered through a 0.2-μm filter into 500-mL glass bottles, which were pre-treated with 1 mL of saturated $HgCl_2$ solution. Water for $\delta^{13}C_{DOC}$ and $\Delta^{14}C_{DOC}$ analyses was collected through a 0.2-μm filter into 250-mL glass bottles sealed with PTFE-lined caps. For gas sampling, water and gas were directed to an inverted graduated funnel via plastic tubing. Gas samples for compositional and isotopic analyses were collected from the top of the inverted beaker or from a gas stripper using a 50-mL gas-tight syringe. Gas was transferred to 160-mL borosilicate vials that had been evacuated to 133.3 Pa. The vials had been pre-treated with 100 μL of saturated $HgCl_2$ solution and sealed with blue butyl rubber stoppers that had been pre-boiled in 1 N NaOH for 45 min. During gas sampling, the gas and water flow rates were measured. Samples for PLFA analysis were collected using carbon-free, Al$(OH)_3$-coated glass wool filters that capture microbial cells through electrostatic interactions (Mailloux et al., 2012). The lipid cartridges were packed with Al$(OH)_3$-coated glass wool and combusted for 24 h at 450 °C prior to sampling (Mailloux et al., 2012). Two lipid filter cartridges were directly connected to the side valves of the stainless steel manifold and water was allowed to flow through the lipid cartridges for up to several weeks, depending on mining operations, at a rate of 0.5–1 L min^{-1}. Since the filtration periods differed from sample to sample, flow accumulators were used to record the total volumes of filtered water through each cartridge. At such high flow rates, the geochemical conditions within the filter cartridges should be similar to the native borehole water being sampled and any geochemical processes and substrates being mediated and utilized, respectively, by the communities would be the same within the filter as in the fracture zone. Immediately upon collection, the cartridges were placed in a cooler of blue ice, either on site or immediately upon reaching the surface. The filter material was then aseptically removed from the cartridges and transferred into double Whirl-pak® bags (sterile from the manufacturer) and stored at −80 °C at the University of the Free State until processing. A dry-shipper (model MVE XC20/3) was used to transport the filter materials to McMaster University at liquid N_2 temperature.

2.3. PLFA extraction and composition analysis

All Al$(OH)_3$-coated glass wool filters were freeze-dried prior to extraction. PLFAs were extracted twice from each filter material using a modified Bligh and Dyer (1959) method. The resulting extracts were separated via silica gel chromatography into non-polar, neutral and polar fractions, using different organic solvents – hexane and dichloromethane (DCM) for non-polar fractions, acetone for neutral fractions, and methanol for polar fractions (Guckert et al., 1985). Phospholipids recovered from the polar fractions were then converted to fatty acid methyl esters via mild-alkaline methanolysis and subsequently purified by a secondary silica gel chromatography to remove residues of non-polar and neutral fractions using 4:1 hexane:DCM, DCM and methanol (Guckert et al., 1985). PLFAs were identified and quantified using Agilent 6890 gas chromatography-mass spectrometry (GC–MS) (Agilent Technologies Inc., Santa Clara, CA, USA). Samples BE326 Bh1 and BE326 Bh2 were analyzed in 2011 with a HP-88 column and a temperature program of 80 °C (hold 1 min), 10 °C/min to 175 °C (hold 12 min), 2 °C/min to 190 °C (hold 10 min), and 10 °C/min to 230 °C (hold 10 min). Samples DR5IPC, TT107, TT109 Bh2 and KL445 were measured in 2012 with a DB-5MS capillary column (30 m × 0.25 μm film thickness) with a temperature program of 50 °C (hold 1 min), 20 °C/min to 130 °C, 4 °C/min to 160 °C, and 8 °C/min to 300 °C (hold 5 min). PLFAs were identified based on their retention times and mass fragmentation patterns and compared to known standards (Bacterial Acid Methyl Esters Mix, Matreya Inc., Pleasant Gap, Pennsylvania, USA). PLFAs were quantified based on the closest chain length(s) from a series of external standard curves created for C14:0, C16:0, C18:0 and C20:0.

Fatty acid identities are listed with the following nomenclature: total number of carbon atoms followed by the total number of double bonds (e.g., 16:1 represents a 16-carbon monounsaturated fatty acid). Terminal-branching fatty acids are indicated by the prefixes *i* (*iso*) and *a* (*anteiso*). Mid-branching positions are represented by the number of carbon atoms from the carboxyl group to the methyl group (e.g. 10Me16:0). Cyclopropyl fatty acids are represented by the prefix *cy*.

2.4. Cellular abundance

For direct cell counting, 45 mL of unfiltered fracture water was fixed with sterile formaldehyde (final concentration, 4% v/v) and filtered through a sterile 0.22 μm Millipore GTTP-type membrane filter. Cell counts for BE326 Bh1 and BE326 Bh2 were performed at the University of Delaware using a SYBR Gold nucleic acid stain and epifluorescence microscopy. Direct cell counts were performed for 15 fields of view, and an average was taken of these values. Microbial cell counts of fracture water collected from the other sample sites were performed at the University of the Free State using a DAPI stain (Porter and Feig, 1980) and fluorescence microscopy. Direct cell counts were performed for 20 fields, and an average was taken of these values.

PLFA concentrations were converted to microbial cell abundances based on a conversion factor of 6×10^4 cells per picomole PLFA (Green and Scow, 2000), which was applied to the sum of the molar concentrations of each PLFA identified in a sample. This conversion factor was adopted under the assumption that, in subsurface sites, the microorganisms are nutrient-deprived and thus small. The comparison of amino acid abundance with cell counts from South African fracture water is consistent with this assumption (Onstott et al., 2014). Taking into account the total volume of water filtered during sampling, the cell abundance was converted into a concentration of cells per mL. For samples where only a portion of the filter extract was analyzed for PLFAs (DR5IPC: 9/10th, TT107: 9/10th, TT109 Bh2: 1/10th), the observed mass of extracted PLFAs was scaled up to generate a cell concentration that would have been expected in the total volume of water filtered.

Because of the uncertainties in the conversion factor, the collector efficiency of the filters, the non-uniform distribution of cells in the filters, temporal variations in the cell concentrations, the presence of Archaea and Eukaryota in the microbial community and the total volume of water filtered, the cell count data and the PLFA-based bacterial abundance results are not expected to be precisely the same.

2.5. $\delta^{13}C$ analyses of PLFA, DIC, DOC and CH_4

The $\delta^{13}C$ compositions of the PLFAs and potential carbon sources (DIC, DOC and CH_4) are referenced to the internationally accepted standard carbonate rock Vienna Pee Dee Belemnite (PDB) and reported in the standard $\delta^{13}C$ notation (Sessions, 2006):

$$\delta^{13}C_{sample} = \frac{(R_{sample} - R_{std})}{R_{std}} \times 1000 \quad (1)$$

where R_{sample} and R_{std} are the $^{13}C/^{12}C$ isotope ratios of the sample and standard, respectively. $\delta^{13}C_{PLFA}$ values were measured using gas chromatography–isotope ratio mass spectrometry (GC–IRMS). Aliquots of microbial PLFAs were injected into a split/splitless injector set to splitless mode at 300 °C prior to separation on an Agilent 6890 GC–MS (as described in Section 2.3). Individual PLFAs were combusted to CO_2 as they eluted from the column via a combustion oven set at 960 °C. The evolved CO_2 was analyzed using a Delta^{Plus} XP continuous flow IRMS. Only PLFAs with sufficient peak amplitude and baseline chromatographic resolution were analyzed for $\delta^{13}C$. Isotopically characterized methanol was used for mild alkaline methanolysis. To account for the addition of one methyl group per fatty acid, $\delta^{13}C_{PLFA}$ values were corrected using the following equation:

$$\delta^{13}C_{PLFA} = \frac{[(N+1) \times \delta^{13}C_{measured} - \delta^{13}C_{MeOH}]}{N} \quad (2)$$

where N is the number of carbon atoms.

DIC and DOC concentrations and their $\delta^{13}C$ compositions were measured on an Aurora 1030 W TOC Analyzer (OI Analytical, USA) at Princeton University. Using 9 mL water samples, the DIC was converted to CO_2 gas by the addition of 0.5 mL of 5% H_3PO_4 solution for 2 min at 70 °C. The DOC remaining in the sample was then oxidized to CO_2 by the addition of 1–1.5 mL of 10% $Na_2S_2O_8$ solution for 2.5–6 min at 98 °C. In both instances, the CO_2 was purged using high purity N_2 gas and the CO_2 was measured using a solid-state non-dispersive infrared (SSNDIR) detector. Gas compositions and CH_4 $\delta^{13}C$ compositions were measured independently using GC–IRMS at University of Toronto and gas chromatography (Peak Performer 1 series, Peak Laboratories, USA) at Princeton University. The GC–IRMS system was composed of a Varian 3400 capillary gas chromatogram and an oxidation oven at 980 °C interfaced directly to a Finnigan 252 gas source mass spectrometer, and a temperature program of 35 °C (hold 6 min), 30 °C/min to 110 °C (hold 0 min), and 5 °C/min to 220 °C (hold 5 min) was used. The accuracy and reproducibility for $\delta^{13}C$ analysis was ±0.5‰ for DIC, DOC, CH_4 and PLFA, unless reported otherwise.

2.6. $\Delta^{14}C$ analysis of PLFA, DIC and CH_4

CH_4 for $\Delta^{14}C$ analysis was separated on a Varian 3300 GC equipped with a 6-m packed molecular sieve (60 Å) and combusted to CO_2 via the method described in Slater et al. (2006). The $\Delta^{14}C$ analysis of the DIC was performed via accelerator mass spectrometry (AMS), at the National Ocean Sciences Accelerator Mass Spectrometer (NOSAMS) facility at Woods Hole Oceanographic Institution, by acidification and collection of the CO_2 generated as per methods described by McNichol et al. (1994). The concentration of the DIC was also determined and compared to that measured by the procedures in Sections 2.5 and 2.7.

Due to the very low abundances of PLFAs detected in these samples, the mass of carbon in individual PLFAs were below the minimum mass required for $\Delta^{14}C$ analysis by AMS. Therefore, PLFAs extracted from each site were analyzed as bulk samples. Bulk PLFA samples were combusted to CO_2 and converted to graphite for $\Delta^{14}C$ analysis via AMS at NOSAMS. To account for the addition of one methyl group per fatty acid (from mild alkaline methanolysis), $\Delta^{14}C_{PLFA}$ values were corrected using the following equation:

$$\Delta^{14}C_{PLFA} = \frac{[(N+1) \times \Delta^{14}C_{measured} - \Delta^{14}C_{MeOH}]}{N} \quad (3)$$

In this case, N is the average number of carbon atoms for a set of PLFAs. The accuracy and reproducibility for $\Delta^{14}C$ analysis was ±10‰ for DIC and CH_4 and ±20‰ for PLFA, unless noted otherwise.

The uncorrected radiocarbon age of the DIC was calculated from the $\delta^{13}C$-corrected Fraction Modern (*Fm*) using the following formula,

$$^{14}C\ Age = -8033 \ln(Fm) \quad (4)$$

where 8033 is the reciprocal of the decay rate in years and *Fm,* reported by NOSAMS, is the deviation of the $^{14}C/^{12}C$ ratio of the sample relative to 95% of the radiocarbon concentration of NBS Oxalic Acid I.

To correct for dead carbon addition to the DIC, for instance due to dissolution of the Transvaal Supergroup

dolomite during groundwater recharge, we utilized the following relationship

$$q = \frac{[\mathrm{DIC}]_{\mathrm{recharge}}}{[\mathrm{DIC}]} = \frac{(\delta^{13}\mathrm{C}_{\mathrm{DIC}} - \delta^{13}\mathrm{C}_{\mathrm{dolomite}})}{(\delta^{13}\mathrm{C}_{\mathrm{recharge}} - \delta^{13}\mathrm{C}_{\mathrm{dolomite}})} \quad (5)$$

to calculate the correction factor, q, where $[\mathrm{DIC}]_{\mathrm{recharge}}$ is the DIC concentration at recharge, [DIC] is the DIC concentration in the studied samples, $\delta^{13}\mathrm{C}_{\mathrm{DIC}}$ is the $\delta^{13}\mathrm{C}$ of the DIC in the studied samples, $\delta^{13}\mathrm{C}_{\mathrm{dolomite}}$ is the $\delta^{13}\mathrm{C}$ of the dolomite, and $\delta^{13}\mathrm{C}_{\mathrm{recharge}}$ is the $\delta^{13}\mathrm{C}$ of the DIC at recharge (Clark and Fritz, 1997). Bau et al. (1999) reported $\delta^{13}\mathrm{C}$ values of the Transvaal Supergroup dolomite ranging from 0.51‰ to 0.64‰. Bredenkamp and Vogel (1970) reported $\delta^{13}\mathrm{C}$ values of tritium-bearing groundwater collected from wells penetrating the unconfined Transvaal Supergroup dolomite that ranged from −5.4‰ to −8‰. We also used the Mg^{2+} concentration to estimate the maximum amount of dolomite that dissolved in the fracture water with the following relationship,

$$q = \frac{[\mathrm{DIC}] - 2[\mathrm{Mg}^{2+}]}{[\mathrm{DIC}]} \quad (6)$$

These q values were then used to calculate the corrected ^{14}C age for the DIC utilizing the following equation (Clark and Fritz, 1997),

$$\text{Corrected } ^{14}\mathrm{C\ Age} = -8033 \ln\left(\frac{a^{14}C_{\mathrm{DIC}}}{q a_0{}^{14}C}\right) \quad (7)$$

where $a^{14}\mathrm{C}_{\mathrm{DIC}} = [(\Delta^{14}\mathrm{C}_{\mathrm{DIC}}/10^3) - 1]/e^{(0.00012097(1950\text{-}2011.5))}$, $a_0{}^{14}\mathrm{C} = [(\Delta^{14}\mathrm{C}_{\mathrm{recharge}}/10^3) - 1]/e^{(0.00012097(1950\text{-}1970))}$, $\Delta^{14}\mathrm{C}_{\mathrm{DIC}}$ is the $\Delta^{14}C$ value of the studied samples and $\Delta^{14}\mathrm{C}_{\mathrm{recharge}}$ is the $\Delta^{14}C$ value of tritium-bearing groundwater, which for wells penetrating the Transvaal Supergroup dolomite ranged from −202‰ to 187‰ (Bredenkamp and Vogel, 1970).

The *in situ* rate of autotrophic methanogenesis was estimated from a steady-state first order rate assumption and the $\Delta^{14}C$ of the DIC and CH_4 using the following equation,

$$k_{\mathrm{methanogenesis}} = \lambda \frac{[^{14}C_{\mathrm{CH_4}}]}{[^{14}C_{\mathrm{DIC}}]} \quad (8)$$

where $k_{\mathrm{methanogenesis}}$ is the autotrophic methanogenic first order rate constant (yr^1), λ = the rate of ^{14}C decay = $1.245 \times 10^{-4}\ \mathrm{yr}^{-1}$ and $[^{14}C_{\mathrm{CH_4}}]$ and $[^{14}\mathrm{C}_{\mathrm{DIC}}]$ are the ^{14}C concentrations of the CH_4 and DIC (Molar). The *in situ* rate of autotrophic methanogenesis is then given by $k_{\mathrm{methanogenesis}}$ [DIC] in M yr^{-1}.

2.7. Geochemical analyses

The DIC concentration was determined using a Shimadzu TOC-VCSH carbon analyzer at New Mexico Institute of Mining and Technology. The sample was acidified to a pH of 2 with 2 M HCl and sparged with high purity air to remove the CO_2, which was then measured by a non-dispersive infrared detector (NDIR). The sample was then injected into the combustion furnace at 680 °C to convert the DOC into CO_2 gas, which was then measured by the NDIR. The concentrations of anions, including low molecular weight organic acids, were measured by an ion chromatograph coupled to an ESI-quadrapole mass spectrometer (Dionex IC25 and Thermo Scientific MSQ, USA) at Princeton University. The cation concentrations were determined by inductively-coupled-plasma optical emission spectroscopy, ICP-OES (Perkin Elmer Optima 4300 DV, USA) at Princeton University (Lau et al., 2014). The total dissolved salinity was determined by summing the molar concentrations of cations, anions and DIC.

2.8. δ^2H and $\delta^{18}O$ analysis of H_2O

Hydrogen and oxygen isotopic compositions of water samples were determined at the University of Toronto. The $\delta^2\mathrm{H}_{\mathrm{H2O}}$ was determined via manganese reduction at 900 °C using a modified method from Coleman et al. (1982). $\delta^{18}\mathrm{O}_{\mathrm{H_2O}}$ was analyzed using the CO_2 equilibration method of Epstein and Mayeda (1953) and Fritz et al. (1986).

2.9. Molecular analyses

Fracture water was also sampled for DNA analyses. Information regarding sampling, DNA extraction and sequencing has been detailed in Magnabosco et al. (2014) for 16S rRNA gene amplicons and in Lau et al. (2014) for metagenomes. The relative abundance of archaea and bacteria was estimated for BE326 Bh2 (MG-RAST Accessions 4536100.3 and 4536472.3), DR5IPC (MG-RAST Accession 4536473.3), TT107 (MG-RAST Accession 4529964.3) and TT109 Bh2 (MG-RAST Accession 4536476.3) using metagenomic data in order to preclude primer biases. Unassembled sequences of metagenomes were annotated using the lowest common ancestor (LCA) algorithm in MG-RAST (Meyer et al., 2008). A more detailed description of the taxonomic distribution within the archaeal and bacterial domains was obtained through sequencing of the 16S rRNA gene V6 hypervariable (V6) region (NCBI BioProject PRJNA 263371). Although the relative abundances of individual taxonomic groups are subjected to primer biases, the biases would be manifested in all six samples and cross-sample comparison within this study would identify the variations in taxonomic distribution. 16S rRNA gene V6 amplicons were not available for TT107 and, consequently, LCA annotation of the unassembled metagenome was used to estimate the diversity at the lower taxonomic levels. The functional identity of unassembled sequences of metagenomes was assigned using MG-RAST. Here, sequences were first clustered at 90% amino acid (aa) identity and a similarity search was performed on representative sequences (the longest sequence in each cluster) against the database of hierarchical classifications of Kyoto Encyclopedia of Genes and Genomes (KEGG; last updated on Nov 22, 2011). The following search criteria were used: maximum e-value of $1e^{-5}$, minimum identity of 60 %, and minimum alignment length of 15 aa (but 25 aa for TT107) to cover approximately 45% of the sequence length. Since sequences may be assigned with multiple functional annotations, abundance of functional features was calculated by normalizing the number of annotations (instead of sequences) per

category to the total number of annotations. The total number of annotations did not include those classified into Human Diseases and Organizational Systems. Annotations indicative of methanogenesis, CH_4 oxidation and autotrophic carbon fixation were screened for key enzymes. The latter includes the reductive pentose phosphate cycle, reductive tribcarboxylic acid (TCA) cycle, reductive acetyl-CoA pathway, 3-hydro xypropionate (3-HP) bicycle, 3-hydroxy propionate/4- hydroxybutyrate (3-HP/4-HB) cycle and dicar boxylate/4-hydroxybutyrate (DC/4-HB) cycle (Hügler and Sievert, 2011).

3. RESULTS

3.1. Temperature, salinities, pH and pe values

Water temperatures increased with depth, ranging from 26.8 to 38.1 °C at 1 to 1.4 kmbls (DR5IPC and BE326) and 48.7 to 54.5 °C at 3.1 to 3.3 kmbls (Tau Tona and KL445). Salinity was relatively low (TDS 0.19 to 0.3 ppt) in DR5IPC, TT107 and TT109 Bh2, despite the >3 km depths of the latter two boreholes. BE326 Bh1, BE326 Bh2 and KL445 had salinities more than an order of magnitude higher (TDS 3.41–11.1 ppt). The pH and pe values for the four sites ranged from relatively neutral and sub-oxic for the dolomite water sample (DR5IPC) to more alkaline and reducing for the remaining sites (Table 1). This range of values is consistent with those reported by Onstott et al. (2006), who reported pH and pe values of 7 to 8 and 1 to 12, respectively, for the dolomitic water, and pH and pe values of 8 to 9.5 and 0 to −3, respectively, for the deeper fracture waters.

3.2. δ^2H and $\delta^{18}O$ values

The relationships between the fracture water $\delta^{18}O$ and δ^2H values and the Global Meteoric Water Line (GMWL) appeared to trend, in part, with depth (See Table 1, Supporting Information). The shallower sites, DR5IPC and BE326, had $\delta^{18}O$ and δ^2H values that plotted on or near the GMWL. TT107 and TT109 Bh2 plotted slightly above the GMWL, and the deepest site, KL445, plotted well above the GMWL.

3.3. Dissolved species

DR5IPC contained the highest DIC concentration (2400 μM), consistent with the fact that it was from a dolomite aquifer. DIC concentrations were lowest in KL445 (90 μM), and were intermediate in the other samples (330–740 μM; Table 1). With the exception of KL445, the DOC concentrations were all less than the DIC concentrations and below 100 μM. The range of DOC concentrations in this study is somewhat less than those reported by Onstott et al. (2006), which is likely due to the organically cleaner protocols utilized in this study. The DOC concentrations obtained from the Shimadzu TOC-VCSH tended to agree with, or were slightly greater than, those determined by Aurora 1030 W. Because this may indicate that the DOC is somewhat recalcitrant to $Na_2S_2O_8$ oxidation, the DOC concentrations from the Shimadzu TOC-VCSH are reported in

Table 1
Sample information, mines, depths, geochemical parameters, and concentrations of dissolved species (μM).

Sample	Mine	Depth (kmbls)	T (°C)	pH	TDS (ppt)	pe	O_2 (μM)	DIC (μM)	DOC (μM)	Formate (μM)	Acetate (μM)	CH_4 (μM)	C_2H_6 (μM)	C_3H_8 (μM)	n-C_4H_{10} (μM)	i-C_4H_{10} (μM)
DR5IPC	Driefontein	1.05	26.8	7.4	0.19	3.0	1.9	2400	85	34	2.2	26	<0.33	<0.2	<0.1	<0.5
BE326 Bh2 (2011)	Beatrix	1.33	36.9	8.8	4.47	−1.6	<0.3	510	16	8.4	1.6	2000	1.6	0.17	<0.1	<0.5
BE326 Bh2 (2012)	Beatrix	1.33	38.1	8.6	3.59	−1.4	9.4	330	29	0.44	<0.7	900	<0.19	<0.15	<0.1	<0.5
BE326 Bh1	Beatrix	1.33	31.6	9.4	3.41	−0.8	<0.3	390	n.d.	<2.2	0.07	560	<0.1	<0.1	<0.1	<0.5
TT109 Bh2	Tau Tona	3.14	48.7	7.6	0.30	−0.3 to −1.0	6.3	740	39	0.99	0.16	2300	100	13	2.0	0.9
TT107	Tau Tona	3.05	52.1	8.6	0.20	−0.9 to −2.1	6.3	570	18	8.0	0.34	8800	140	20	30	1.8
KL445	Kloof	3.28	54.5	8.0	11.1	−0.8	78	90	410	0.89	28	5500	180	21	24	1.1

Abbreviations: TDS, total dissolved salinity; pe, redox potential, n.d. – not determined.
Propanoate was below detection (<1.4×10^{-6} M).
Lactate was below detection (<5×10^{-7} M), with the exception of BE326 Bh2 (2012), which yielded 1 μM.

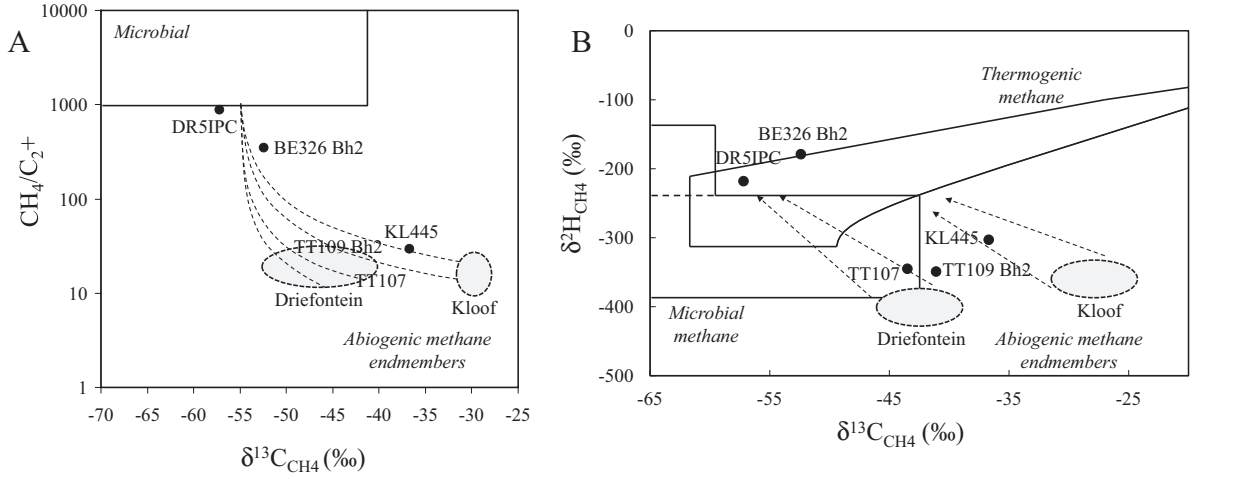

Fig. 1. (A) Plot of CH_4 $\delta^{13}C$ values versus CH_4/C_2^+ ratios, adapted from Hunt (1996) and Sherwood Lollar et al. (2006) illustrating the relatively greater presence of suggested abiogenically produced CH_4 sources in TT107, TT109 Bh2 and KL445. The hatched ovals represent the previously observed ^{13}C-enriched CH_4 suggested to be predominantly abiogenic in origin by Sherwood Lollar et al. (2006) and Ward et al. (2004) from Driefontein and Kloof mines. The dashed lines represent the general trend of mixing lines between points within these ranges and a microbial end-member with a $\delta^{13}C$ of −55‰ (mean of DR5IPC and BE326 Bh2). (B) δ^2H and $\delta^{13}C$ values for CH_4 compared to the conventional fields for microbial and thermogenic CH_4 (after Schoell, 1988) illustrating the relatively greater presence of abiogenically produced CH_4 sources in TT107, TT109 Bh2 and KL445. Hatched ovals represent the ranges observed for suggested abiogenically dominated CH_4 end-members by Sherwood Lollar et al. (2006) and Ward et al. (2004) for Driefontein and Kloof mines. Dashed arrows represent the general trend for mixing lines between points within these ranges, and microbially dominated methane end-members represented by DR5IPC and BE326 Bh2.

Table 1. In all samples, the total organic acid concentrations were significantly less than the DOC concentrations. While lactate and propionate were mostly below detection (<1 μM), formate and/or acetate comprised a significant fraction of the DOC at most sites. Formate comprised 44% of the DOC from TT107, and acetate comprised 14% of the DOC from KL445. The CH_4 concentrations were tens of μM in the dolomite water (DR5IPC) and at mM levels in the deeper fractures, consistent with the CH_4 concentrations of Onstott et al. (2006). C2–C4 alkanes were only detected in the deeper boreholes and CH_4/C_{2+} ratios (Fig. 1a; Table 1 SI) were more than an order of magnitude higher in the shallower boreholes than the deeper boreholes. Dissolved O_2 was measured at either μM concentrations or below detection for all sites, with the exception of KL445. At KL445, the elevated O_2 levels were likely due to air contamination during sampling due to a leaky borehole casing.

3.4. $\delta^{13}C$ values

Two groups of $\delta^{13}C_{DIC}$ values were observed: highly ^{13}C-depleted values (−42.6‰ to −32.0‰) from BE326 Bh1, BE326 Bh2 and KL445 and less ^{13}C-depleted values (−9.3‰ to −5.0‰) from DR5IPC, TT107 and TT109 Bh2 (Fig. 2). Notably, this grouping of boreholes is distinguished by their salinities, with the more ^{13}C-depleted values corresponding to higher salinities. The $\delta^{13}C_{DOC}$ values ranged from −28‰ to −43‰ (with the exception of KL445 which yielded a $\delta^{13}C_{DOC}$ of −155‰, the

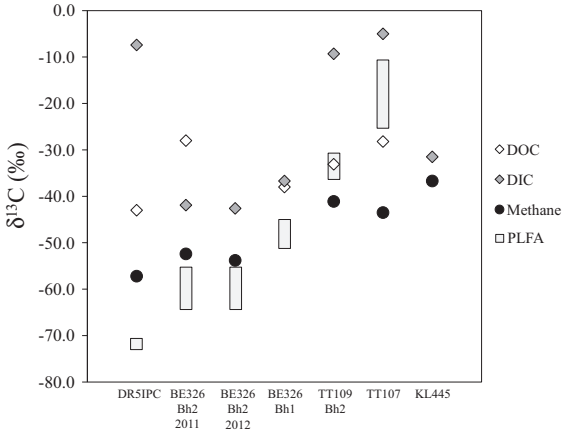

Fig. 2. $\delta^{13}C$ values for DOC, DIC, CH_4 and PLFAs from six deep subsurface fracture water sites. PLFA $\delta^{13}C$ values are ranges measured for the total set of fatty acids identified at each site. KL445 did not contain sufficient carbon from PLFA to measure $\delta^{13}C$. KL445 $\delta^{13}C_{DOC} = -155‰$ was not plotted due to uncertainty regarding reliability. The calibration of the CRDS used for this analysis was not valid this far from the standard used ($\delta^{13}C = -27‰$) and was very close to the detection limit for the CRDS. Further, the concentration of DOC determined by the CRDS was only 20% of that determined by combustion analysis at NMIT, raising concern that the high salinity of this sample relative to the other samples affected the persulfate oxidation used for the CRDS analysis. Such an affect may have reduced observed concentrations and/or fractionated the resulting $\delta^{13}C_{DOC}$ value. Low gas levels precluded the $\delta^{13}C$ analysis of CH_4 at Be326 Bh1.

reliability of which was uncertain due to the difficulties with DOC isotopic analysis of that sample – see figure heading for further discussion) and did not correlate with the $\delta^{13}C_{DIC}$ values or depth (Fig. 2). The $\delta^{13}C_{CH4}$ values were generally more depleted in the shallower boreholes, ranging from −52.1‰ to −57.8‰ in BE326 Bh1, BE326 Bh2 and DR5IPC. In the deeper boreholes, KL445 and TT107 and TT109 Bh2, $\delta^{13}C_{CH4}$ ranged from −36.7‰ to −41.1‰. The $\delta^{2}H_{CH4}$ values were separated in a similar fashion with the shallower boreholes being heavier ($\delta^{2}H_{CH4} = -218$‰ to −179‰) than the deeper boreholes ($\delta^{2}H_{CH4} = -349$‰ to −303‰) (Fig. 1b; Table 1 SI). The $\delta^{13}C_{PLFA}$ values were likewise generally more depleted in the shallower boreholes, ranging from −72.9‰ to −45.1‰ in BE326 Bh1, BE326 Bh2 and DR5IPC. In the deeper boreholes, TT107 and TT109 Bh2, the $\delta^{13}C_{PLFA}$ ranged from −36.3‰ to −11.0‰. The collected biomass was insufficient to determine the $\delta^{13}C_{PLFA}$ in KL445 (Figs. 2 and 3).

3.5. $\Delta^{14}C$ values

$\Delta^{14}C_{DIC}$ values were highly depleted ($\Delta^{14}C_{DIC}$ −863‰ to −987‰) with the exception of TT107 ($\Delta^{14}C_{DIC} = -497$‰; Fig. 4). Based on equation 4, the uncorrected ages

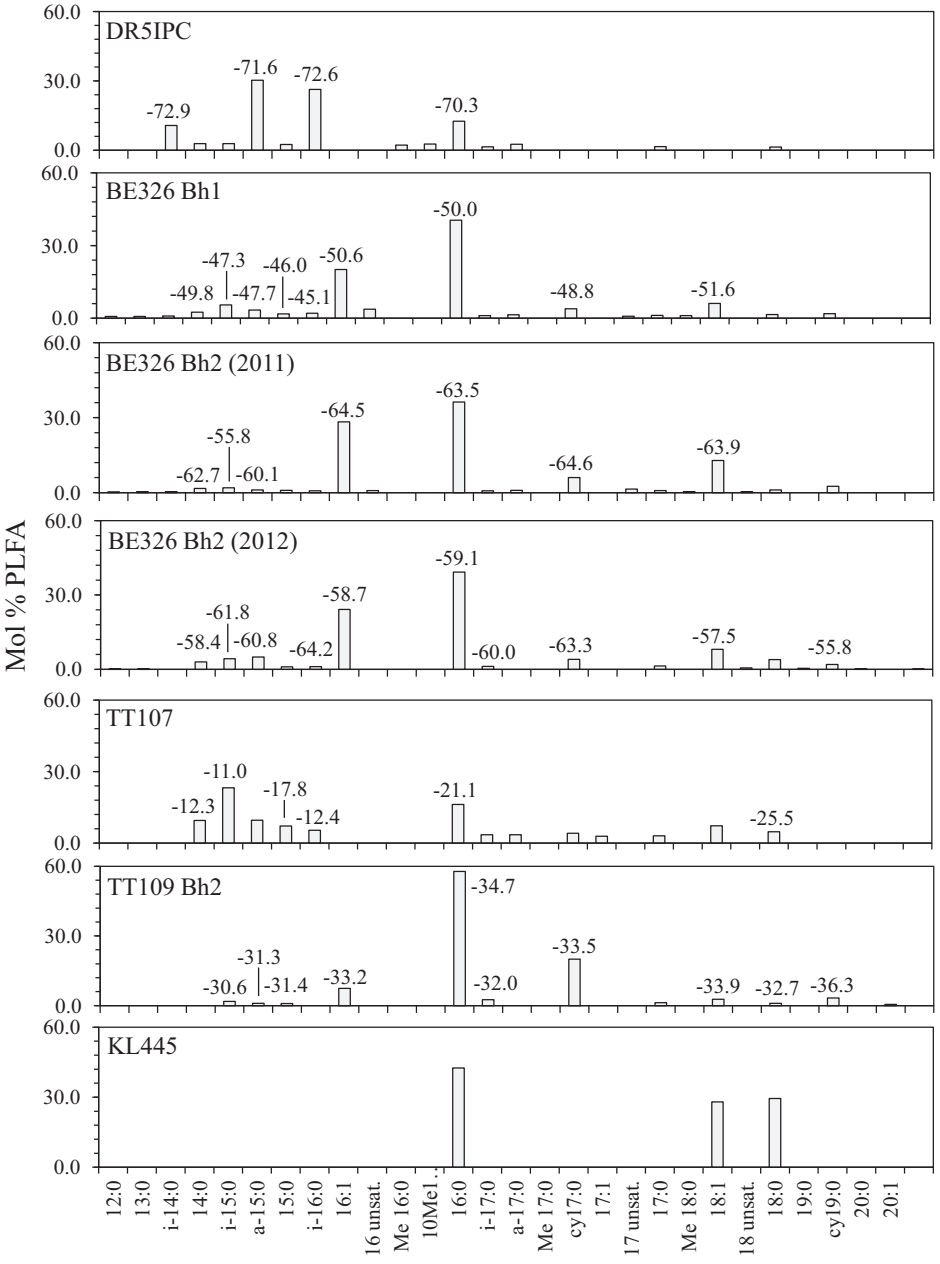

Fig. 3. Relative abundances (mol%) and $\delta^{13}C$ values (‰) of individual PLFAs sampled from the six deep subsurface fracture systems. $\delta^{13}C_{PLFA}$ values only include PLFAs of sufficient mass for $\delta^{13}C$ analysis.

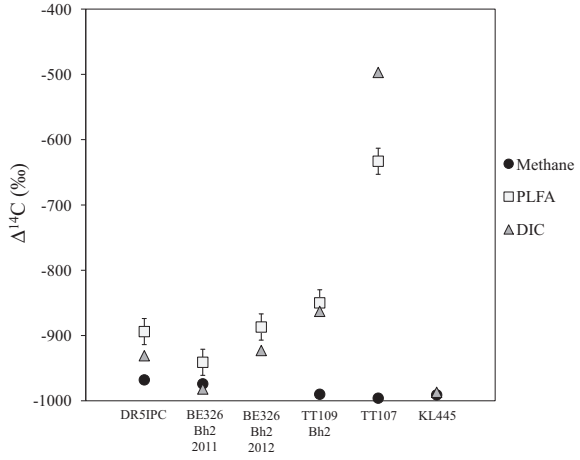

Fig. 4. $\Delta^{14}C$ values for DOC, DIC, PLFA and CH_4 from six deep subsurface fracture water sites.

for the DIC ranged from 5.45 kyr for TT107 to 32.4 kyr for BE326 Bh2 2011 (Table 2). The geochemical data for DR5IPC, TT107 and TT109 Bh2 are consistent with dissolution of carbonate and, using Eqs. (5)–(7), the corrected ages for TT107 range from 1.4 to 5.7 kyr, whereas the corrected ages for TT109 Bh2 and DR5IPC were indistinguishable and range from 16 to 23 kyr (Table 2). With the exception of BE326 Bh2 2011, all of the $\Delta^{14}C_{CH4}$ values were more depleted than their corresponding $\Delta^{14}C_{DIC}$ values (Fig. 4). $\Delta^{14}C_{PLFA}$ values were generally slightly enriched in ^{14}C relative to the corresponding $\Delta^{14}C_{DIC}$ values, with the exception of TT107, which was depleted in ^{14}C relative to DIC but enriched relative to the $\Delta^{14}C_{CH4}$. Unfortunately, reliable $\Delta^{14}C_{DOC}$ values could not be obtained for these samples.

3.6. Microbial abundance

Direct cell counts tended to be lower than the cellular abundances derived from PLFA concentrations (Fig. 4). This may be due to several factors including: potential variations in cellular abundances over the long deployment of the PLFA filters not being captured by direct counting; the fact that a generic conversion factor was used to convert PLFA concentrations to cell abundances; and variations in the distribution of biomass on the glass wool filter. However, these results fell within the range of PLFA values and cell concentrations for previous fracture water samples from the Witwatersrand Basin (Pfiffner et al., 2006), with the exception of KL445, which is an order of magnitude lower than the lowest previous data. The low concentrations of PLFAs extracted from KL445, in conjunction with the lack of amplification of DNA from this site, suggested that some factor inhibited successful detection of the cells observed during cell counting using these two approaches. It was not clear what this factor was, but the low yield precluded further analysis of PLFA distributions or genetic data for this sample. There was no discernible reason why PLFA-derived cell abundances for TT109 Bh2 were notably higher than the direct count results. The cell abundances did not show any strong evidence of correlation with depth or geochemistry, consistent with the previously published cell concentrations for fracture water from the Witwatersrand Basin (Onstott et al., 2010). The interpretation of the total microbial community biomass abundance from just the planktonic cellular concentrations is confounded by the fact that sessile microorganisms undoubtedly exist in patches on the fracture surfaces (Wanger et al., 2006) and these may become entrained to varying degrees into the fracture water flow from the borehole.

3.7. Microbial community composition

3.7.1. Metagenomic assessment

The whole-genome shotgun metagenomic data indicated that bacteria dominated the microbial communities (>95%) (Table 3). DR5IPC contained the largest archaeal proportion; however, even then, the archaea-related sequences comprised only 4.6% of the sequences in DR5IPC's metagenome. As revealed by the 16S rRNA gene amplicon sequencing, *Proteobacteria* were the most abundant bacterial phylum within BE326 Bh2, DR5IPC, and TT109 Bh2, whereas the unassembled TT107 metagenome was dominated by *Firmicutes*-related sequences. Together, type I and type II methanotrophs accounted for a low percentage (<3%) of each site's bacterial community (Table 3). No methanotrophs were identified in TT107, whereas TT109 Bh2 contained the highest percentage of

Table 2
^{14}C DIC model ages and rates of methanogenesis.

Sample	Uncorrected ^{14}C age (kyr)	Model ^{14}C age (kyr)	Autotrophic Methanogenesis Rate (nM/yr)*
DR5IPC	21.3 ± 0.1	16.4–22.9	1.5 ± 0.1
BE326 Bh2 (2011)	20.5 ± 0.1 to 32.4 ± 0.2	n.a.	n.a.
BE326 Bh2 (2012)	19.7 ± 0.1	n.a.	n.a.
BE326 Bh1	20.3 ± 0.1	n.a.	n.a.
TT109 Bh2	16.0 ± 0.1	16.3–21.9	6.5 ± 0.8
TT107	5.45 ± 0.03	1.41–5.68	8.7 ± 2.3
KL445	34.7 ± 0.3	n.a.	n.a.

Abbreviation: n.a. = not available

* The same calculations performed on data published by Slater et al. (2006) yielded the following rates in nM/yr: Ev219 ED = 180, Dr938 H3 = 38, Be16 GDW = 14, Ev522 CTS = 7.5, and Be39 CTS = 2.2.

Table 3
Relative abundance of Archaea and Bacteria in metagenomic data and proportions of putative methanogens and methanotrophs in the domain-specific 16S rRNA gene amplicon data.

% Microbial group	BE326 Bh2 (2011)	BE326 Bh2 (2012)	DR5IPC	TT109 Bh2	TT107
% Archaea	1.5	1.5	4.6	0.2	3.9
% Bacteria	98.5	98.5	95.4	99.8	96.1
% Methanogens	0.3^	0.3^	0.9^	<0.1^	1.2
% ANME[a]	0.2^	0.1^	<0.1^	<0.1^	n.d.
% Type I Methanotrophs[b]	1.1*	1.5*	0.9*	2.3*	n.d.
% Type II Methanotrophs[c]	0.4*	0.5*	0.1*	0.1*	n.d

n.d. = not determined.
[a] Anaerobic methanotrophic archaea (ANME-1, ANME-2, ANME-3).
[b] Family *Methylococcaceae*.
[c] Family *Methylocystaceae*.
* Adjusted based on percent abundance in bacterial 16S rRNA gene V6 dataset.
^ Adjusted based on percent abundance in archaeal 16S rRNA gene V6 dataset.

methanotrophs. TT107 contained the highest percentage of methanogens (1.2%), whereas BE326 Bh2 contained the highest percentage of anaerobic methanotrophic archaea (ANMEs) (0.1–0.2%). A more detailed discussion of the bacterial diversity of the sites can be found in Magnabosco et al. (2014).

Metagenomic data indicated that the relative abundance of putative enzymes encoding multiple steps in methanogenesis (and archaeal anaerobic methanotrophy) was the largest in TT107, followed by BE326 Bh2, and DR5IPC and TT109 Bh2 (Table 4). No CH_4 monooxygenases were detected, which may be partly explained by the low percentage of aerobic methanotrophic taxa. The reductive acetyl-CoA pathway was the most dominant CO_2 fixation pathway in most samples, ranging from 0.16% to 0.53% of the reads. TT109 Bh2 was exceptional, however, exhibiting a greater diversity in CO_2 fixation pathways with reductive acetyl-CoA pathway comprising 0.16%, the 3-hydroxypropionate/4-hydroxybutyrate (3-HP/4-HB) cycle comprising 0.175%, and the reductive pentose phosphate cycle comprising 0.121%. The 3-HP bicycle was the least common and no annotations belonging to DC/4-HB cycle were detected.

3.7.2. Geochemical (PLFA-based) microbial community assessment

Differences among the individual PLFA profiles of the six boreholes indicate varying community structures and/or microbial responses to environmental stressors (Fig. 5). Unlike the five other boreholes, DR5IPC contained primarily branched PLFAs (79.1 mol%) with *a*-15:0 and *i*-16:0, constituting 30.3 mol% and 26.3 mol%, respectively (Fig. 5). Such a high proportion of branched PLFAs has been interpreted in the past as indicating a high proportion of Gram-positive bacteria, such as *Firmicutes* (Hardwood and Russell, 1984; Kaneda, 1991). The presence of the PLFA 10Me16:0 in DR5IPC, which is often considered an indicator for the sulphate-reducing *Deltaproteobacteria* (Green and Scow, 2000), is consistent with the 16S rRNA gene amplicon data (Magnabosco et al., 2014). Alternatively, it has also been demonstrated to be produced by the anaerobic methanotroph *Ca.* "Methylomirabilis oxyfera" (Raghoebarsing et al., 2006), but no V6 sequences related to *Ca.* "Methylomirabilis oxyfera" or the phylum NC 10 were detected in this sample.

BE326 Bh1 and BE326 Bh2 appeared to contain similar microbial communities based on their PLFA profiles, as the majority of the PLFAs identified in BE326 Bh1 and BE326 Bh2 were common to both systems. This included the short chain PLFAs 12:0, 13:0 and *i*-14:0 of unspecified bacterial origin, which were not identified in the other samples. Both BE326 Bh1 and BE326 Bh2 were dominated by 16:0, followed by the monounsaturated PLFAs 16:1 and 18:1, which are common in Gram-negative bacteria (Green and Scow, 2000). This is consistent with the 16S rRNA gene amplicon profiles, which are dominated by *Proteobacteria* (Magnabosco et al., 2014).

All of the PLFA profiles, except for those of DR5IPC and KL445, contained some cyclopropyl PLFAs. Although cyclopropyl fatty acids are potential indicators for anaerobic bacteria (Fang and Barcelona, 1998; Green and Scow, 2000), they have also been shown to be produced in response to environmental stressors, such as severe nutrient deprivation (Guckert et al., 1986; Kieft et al., 1994). TT109 Bh2, in particular, contains a relatively high proportion of *cy*17:0 (20.0 mol%). Pfiffner et al. (2006) also reported that *cy*17:0 was widely distributed amongst the fracture water samples from the Witwatersrand Basin.

4. DISCUSSION

4.1. Aqueous geochemistry

The observed aqueous geochemistry of these four sites indicated several distinctions. In DR5IPC, the relatively low temperatures, elevated DIC concentrations, low CH_4 concentrations, and agreement with the GMWL were consistent with the fact that it was sampled in a dolomitic aquifer and had experienced little water–rock interaction beyond carbonate dissolution/precipitation (Table 1, Table 1 SI). The isotopically enriched $\delta^{13}C_{DIC}$ (−7.4‰, Fig. 2) was indicative of a system receiving inputs from carbonate dissolution and recycling of organic matter. This is consistent with its location within and beneath the

Table 4
Relative abundance of putative enzymes in methanogenesis and autotrophic carbon fixation pathways detected in metagenomic data. Values in bold font are the relative abundances of each pathway with respect to the total dataset.

Putative pathway	DR5IPC (%)	BE326 Bh2 (2011) (%)	BE326 Bh2 (2012) (%)	TT109 BH2 (%)	TT107 (%)
Methanogenesis	***0.019***	***0.053***	***0.038***	***0.021***	***0.216***
fwd, fmd; formylmethanofuran dehydrogenase subunit A [EC:1.2.99.5]	0.003	0.026	0.016	0.010	0.045
mtr; tetrahydromethanopterin S-methyltransferase [EC:2.1.1.86]	0.005	0.002	0.004	<0.001	0.006
methenyltetrahydromethanopterin cyclohydrolase [EC:3.5.4.27]	<0.001	0.006	0.002	0.002	<0.001
mcr; methyl-coenzyme M reductase[EC:2.8.4.1]	0.004	0.004	0.005	0.001	0.002
mta; methanol-5-hydroxybenzimidazolylcobamide Co-methyltransferase [EC:2.1.1.90]	0.002	0.001	0.001	<0.001	0.106
mtb; [methyl-Co(III) methylamine-specific corrinoid protein]:coenzyme M methyltransferase [EC:2.1.1.247]	<0.001	–	–	–	–
mtd; methylenetetrahydromethanopterin dehydrogenase [EC:1.5.99.9]	<0.001	0.005	0.003	0.004	<0.001
mtt; trimethylamine-corrinoid protein Co-methyltransferase [EC:2.1.1.250]	0.004	0.006	0.005	0.004	0.055
Reductive pentose phosphate cycle	***0.001***	***0.100***	***0.072***	***0.121***	***0.012***
prkB; phosphoribulokinase [EC:2.7.1.19]	0.001	0.100	0.072	0.121	0.012
Reverse tricarboxylic acid (TCA) cycle	***0.006***	***0.096***	***0.072***	***0.009***	***0.0075***
frd; fumarate reductase [EC:1.3.99.1]	0.006	0.096	0.072	0.009	0.0075
Reductive acetyl-CoA pathway	***0.531***	***0.245***	***0.219***	***0.160***	***0.418***
fhs; formate-tetrahydrofolate ligase [EC:6.3.4.3]	0.342	0.115	0.100	0.048	0.276
folD; methylenetetrahydrofolate dehydrogenase/methenyltetrahydrofolate cyclohydrolase [EC:1.5.1.5 3.5.4.9]	0.190	0.130	0.120	0.112	0.142
3-hydroxypropionate (3-HP) bicycle	**–**	***0.003***	***0.002***	***0.002***	***0.004***
smt; succinyl-CoA:(S)-malate CoA transferase [EC:2.8.3.-]	–	<0.001	<0.001	<0.001	<0.001
mct; mesaconyl-CoA C1-C4 CoA transferase	–	<0.001	<0.001	–	<0.001
meh; mesaconyl-C4 CoA hydratase	–	0.003	0.001	0.001	0.004
3-Hydroxypropionate/4-hydroxybutyrate (3-HP/4-HB) cycle	***0.088***	***0.063***	***0.088***	***0.175***	***0.060***
fadN; 3-hydroxyacyl-CoA dehydrogenase [EC:1.1.1.35]	0.088	0.063	0.088	0.175	0.060
4-Hydroxybutyryl-CoA synthetase (4-hydroxybutyrate-CoA ligase, AMP-forming) [EC:6.2.1.-]	<0.001	<0.001	<0.001	<0.001	–

Dashed line = Not detected.

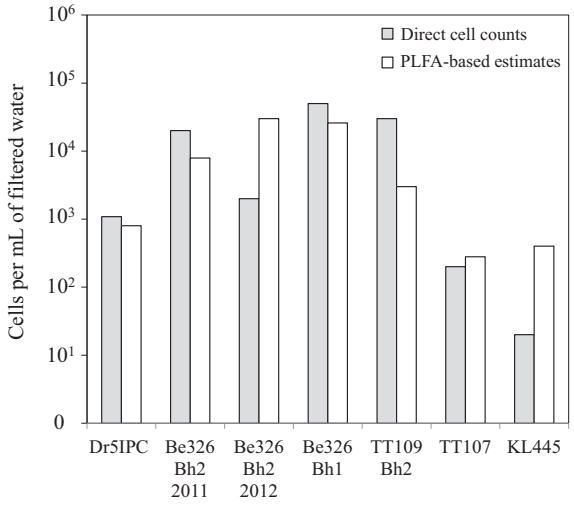

Fig. 5. Estimates for the number of microbial cells per mL of fracture water. Cell estimates displayed as grey bars are based on PLFA concentrations and a conversion factor of 6×10^4 cells per picomole of PLFA (Green and Scow, 2000). Cell density estimates displayed as light grey bars are based on direct cell counts via epifluorescence microscopy.

Transvaal Supergroup dolomites, which contain carbonate veins of similar isotopic composition (Onstott et al., 2006).

In BE326 Bh1 and Bh2, the elevated temperatures, and the increased, but variable, salinity indicated that mixing between paleometeoric water and ancient saline hydrothermal fluid occurs with these fracture systems (Onstott et al., 2006; Table 1, Fig. 2). The very negative $\delta^{13}C_{DIC}$ values (−36.7‰ to −42.6‰) could only be achieved via inputs from the oxidation of CH_4 ($\delta^{13}C = -52‰$ to −54‰). These values are significantly lighter than any reported previously by Onstott et al. (2006), which ranged from −12‰ to −29‰. Furthermore, they are more depleted that the $\delta^{13}C_{DOC}$ (−28‰), the $\delta^{13}C$ values of organic carbon from the Witwatersrand Supergroup quartzite and Ventersdorp Supergroup metavolcanic, which range from −24‰ to −25‰, and the $\delta^{13}C$ of organic carbon from the Kimberley Shale, which ranges from −28‰ to −30‰ (Silver et al., 2012). As can be expected in complex, fractured subsurface environments, there were variations in a number of geochemical parameters over the year interval between sampling events for BE326 Bh2. Many of these variations were minor (<20%) and their magnitudes were within the ranges observed in other fractured rock systems. The largest variations were observed for DOC, organic acid, CH_4 and light hydrocarbon concentrations. As is often the case, the cause of these variations is difficult to constrain. Such variations may be the result of: (1) geochemical variations in the fracture fluid(s) being drained by the borehole; (2) effects resulting from mining activities impacting the system; or (3) potential changes in microbial activity over the time period. Water isotopic compositions shifted away from the global meteoric water line over the year suggesting that (1) might be the most likely explanation. If this were the case, then it may also explain the fact that the slight increase in the $\Delta^{14}C_{DIC}$ was also observed in $\Delta^{14}C_{PLFA}$ indicating that the carbon sources used by the microbial community was tracking the shift.

The deeper (>3 kmbls) samples, TT107 and TT109 Bh2, appear to have received significant inputs from relatively younger DIC and fresh water. Their salinities were relatively low and comparable to DR5IPC (Table 1), and their δ^2H and $\delta^{18}O$ values were relatively close to the GMWL (SI). The $\delta^{13}C_{DIC}$ values from TT107 and TT109 Bh2 (−5.0‰ to −9.3‰) are similar to that of DR5IPC and consistent with what might be expected from ground waters that have received a mixture of inputs from dissolved carbonate and respired organic matter (Fig. 2). Their $\Delta^{14}C_{DIC}$ values were the most enriched in ^{14}C, particularly for TT107 (Fig. 3). These observations are consistent with the fact that these boreholes intersect the same fracture network ~100 m from Jean's dyke, which cuts across the Archean strata. The margins of young dykes in this part of the Tau Tona mining property are known by the mining geologists to contain relatively fresh paleometeoric water.

KL445 appears to have received the greatest input from water–rock interactions. It had the highest observed salinity, low DIC concentrations, isotopically depleted $\delta^{13}C_{DIC}$, and δ^2H and $\delta^{18}O$ values that fell very far from the GMWL (Table 1, Fig. 2, Table 1 SI). The depleted $\delta^{13}C_{DIC}$ is consistent with inputs from oxidation of ^{13}C-depleted organic carbon, as was the case for BE326 Bh1 and BE326 Bh2. All of these indications of KL445 being a more isolated system are consistent with the fact that it intersects Danie's fault, which is late Ventersdorp Supergroup in age and does not offset the overlying dolomite (Manzi et al., 2012). The slightly elevated $\Delta^{14}C$ observed in this borehole is correlated with high O_2 concentrations (Fig. 3, Table 1) indicating that this is likely an artefact caused by dissolution of mine air during sampling due to a leaky borehole casing.

4.2. CH_4 geochemistry

Unlike the aqueous geochemistry, the variations in CH_4 geochemistry were correlated with depth. For both of the shallower sites (DR5IPC and BE326), the $\delta^{13}C$ and δ^2H values of CH_4, and the CH_4/C_{2+} ratios (Fig. 1a, b; Table 1 SI) were consistent with an autotrophic microbial methanogenic origin for the CH_4. In the case of DR5IPC, the large carbon isotope separation of 49.8‰ between $\delta^{13}C_{DIC}$ and $\delta^{13}C_{CH4}$ (Fig. 2), the fact that it contains the highest abundance of methanogens compared to the other sites (Table 3), and the relatively high abundance of *mtr* and *mcr* genes (Table 4) are also consistent with microbial methanogenesis. Metagenomic data also identified the presence of methanogens and *mtr* and *mcr* genes in BE326, though to a lesser extent. This interpretation of the occurrence of autotrophic methanogenesis is consistent with the isotopic geochemistry data previously reported from the Witwatersrand Basin (Ward et al., 2004) and elsewhere (Whiticar, 1999; Londry et al., 2008).

In contrast, the $\delta^{13}C$ and δ^2H values of CH_4 and the CH_4/C_{2+} ratios from the deeper sites (TT107, TT109 Bh2, and KL445) fell within the range of values previously reported from the deeper mines of the Carletonville region

by Sherwood Lollar et al. (2006) and reflect a mixture of abiogenic hydrocarbons mixed with microbially-generated CH_4 (Fig. 1a and b). When the CH_4 isotopic data are considered in combination with the aqueous geochemistry of TT107 and TT109 Bh2, it indicates a mixing of inputs from geologically-isolated fracture fluid containing predominantly abiogenic CH_4, with more paleometeoric influx along Jean's dyke. In KL445, the stronger signals of water–rock interaction (increased salinity, greater offset from the GMWL) suggest that the extent of mixing with paleometeoric water is far less. However, without specific knowledge of the end-members at each site, the extent to which this is true is difficult to constrain.

4.3. Microbial carbon sources and cycling

The $\delta^{13}C$ and $\Delta^{14}C$ results for the PLFAs, DIC and CH_4 indicate that these systems can be divided based on the extent of biological cycling of CH_4. In the shallower systems containing biogenic CH_4 (DR5IPC, BE326 Bh1, BE326 Bh2), there is evidence that this CH_4 was playing a key role in supporting the microbial ecosystem. In contrast, in the deeper systems (TT107, TT109 Bh2), despite the presence of high concentrations of predominantly abiogenic CH_4, any cycling of CH_4 by the *in situ* microbial community is insufficient to create a recognizable isotopic signature.

4.3.1. CH_4 cycling sustains the shallow (<1.3 kmbls) subsurface microbial communities

4.3.1.1. Evidence of the predominant signature of CH_4 cycling in DR5IPC. In the shallower systems studied, the $\delta^{13}C$ depleted PLFAs indicated a key role for CH_4 in supporting the *in situ* microbial ecosystems. In DR5IPC, the only reasonable carbon source for the highly $\delta^{13}C$ depleted PLFAs (−72.9‰ to −70.3‰) is CH_4 oxidation. The PLFAs were negatively offset from $\delta^{13}C_{CH4}$ (-57.2‰) by 14.9–17.5‰, consistent with the KIEs typically involved in microbial uptake of CH_4 (i.e. $\Delta\delta^{13}C_{CH4\text{-}PLFA}$ ranging from 10‰ to 30‰) (Jahnke et al., 1999; Hayes, 2001; Templeton et al. 2006) (Fig. 2). Concurrently, the isotopic separation between DIC and the PLFAs in this borehole ($\Delta\delta^{13}C_{DIC\text{-}PLFA}$ = 62.9‰ to 65.5‰) exceeded the largest autotrophic carbon isotope fractionation observed to date ($\Delta\delta^{13}C_{DIC\text{-}PLFA}$ = 58‰) (Londry et al., 2004). Similarly, the isotopic separation between DOC and PLFAs ($\Delta\delta^{13}C_{DOC\text{-}PLFA}$ = 27‰ to 30‰) was greater than expected for heterotrophy (Londry et al., 2004). And while methanotrophic activity would be expected to introduce isotopically light CO_2 into the DIC pool, the fact that DIC concentrations were two orders of magnitude higher than CH_4 likely swamped this signal, resulting in a limited effect on the $\delta^{13}C$ of DIC.

The $\Delta^{14}C_{PLFA}$ value (−894 ± 8‰) was consistent with microbial utilization of an ancient carbon source such as the CH_4 (−968‰) and the DIC (−930‰) (Fig. 3). However, the $\Delta^{14}C_{PLFA}$ value was slightly enriched in ^{14}C relative to these two carbon pools, indicating some concomitant incorporation of a more modern carbon source or potential temporal variation in $\Delta^{14}C_{DIC}$. The $\Delta^{14}C_{DIC}$ was consistent with the value −933‰ previously reported by Borgonie et al. (2011) from a sample of this borehole collected in 2009, arguing against this latter interpretation. However, another potential source of slightly more ^{14}C-enriched carbon might be the DOC pool. Approximately 45% of the DOC was comprised of formate and acetate (Table 1) and if these were derived from the same recharge zone as the DIC, then its $\Delta^{14}C_{DOC}$ value would be similar to that of the $\Delta^{14}C_{DIC}$ values corrected for carbonate dissolution (−807‰ to −945‰, depending upon the assumed $\Delta^{14}C_{recharge}$).

4.3.1.2. Evidence of CH_4 cycling in combination with other metabolisms in BE326. While similar to DR5IPC, BE326 Bh2 yielded a wider range of $\delta^{13}C_{PLFA}$ values, from −64.6‰ to −55.8‰ in 2011 (Fig. 2 and 3), which remained stable over a year ($\delta^{13}C_{PLFA}$ = -64.2‰ to −55.8‰ in 2012, Fig. 2 and 3). The geochemical conditions and PLFA profiles from BE326 Bh2 were very similar to those of BE326 Bh1, indicating that the two boreholes sampled similar communities. Taking into consideration the various potential carbon sources and the KIEs associated with different metabolisms, the wide range of $\delta^{13}C_{PLFA}$ values in BE326 Bh2 potentially represents evidence of multiple carbon assimilation metabolisms. The most highly ^{13}C-depleted $\delta^{13}C_{PLFA}$ values, representing 14:0, 16:1, 16:0, *cy*17:0, and 18:1, ranged from −62.7‰ to −64.6‰ and were negatively offset from $\delta^{13}C_{CH4}$ by 10.6‰ to 12.5‰, within the range of carbon isotope fractionations typically observed for aerobic methanotrophy, making this the most likely explanation for the observed values ($\Delta\delta^{13}C_{CH4\text{-}PLFA}$ ranging from 10‰ to 30‰) (Jahnke et al., 1999; Hayes, 2001; Templeton et al., 2006). Consistent with this interpretation, the set of PLFAs represented by these highly ^{13}C-depleted values include the unsaturated PLFAs 16:1 and 18:1, isomers of which are considered biomarkers for methanotrophic communities (Gebert et al., 2004; Bodelier et al., 2009; Mills et al., 2010). The occurrence of methanotrophy is further supported by the observed highly depleted $\delta^{13}C_{DIC}$ values (−41.9‰ to −42.6‰), which could only be derived from the oxidation of CH_4 ($\delta^{13}C$ = −52‰ to −54‰) as they are more depleted than the $\delta^{13}C_{DOC}$ and organic carbon in the system (Silver et al., 2012). Unlike in DR5IPC, the CH_4 concentrations in these two boreholes exceed those of DIC by 1.4 to 3.9 times and thus DIC inputs from other sources would not swamp out the signal from CH_4 oxidation. The two remaining PLFAs that were measured for $\delta^{13}C$ from BE326 Bh2 (*i*-15:0 and *a*-15:0) yielded $\delta^{13}C_{PLFA}$ values of −55.8‰ and −60.1‰, with negative offsets from $\delta^{13}C_{CH4}$ ($\Delta\delta^{13}C_{CH4\text{-}PLFA}$ = 3.7‰ and 8.0‰) that are likely too small to result from methanotrophy (Jahnke et al., 1999; Hayes, 2001). Consistent with this observation, *i*-15:0 and *a*-15:0 are generally uncommon in methanotrophic bacteria (Gebert et al., 2004; Bodelier et al., 2009). The $\delta^{13}C$ values of *i*-15:0 and *a*-15:0 were negatively offset from $\delta^{13}C_{DIC}$ by 13.9‰ and 18.2‰, respectively, falling within the range of possible carbon isotope fractionations associated with microbial utilization of DIC, and may indicate acetogenesis, sulphate reduction and/or Fe^{3+} reduction (Ruby et al., 1987; Boschker and Middelburg, 2002;

Londry et al., 2004; Blaser et al., 2013). As was the case for DR5IPC, the carbon isotope separations between these two PLFAs and $\delta^{13}C_{DOC}$ (27.8‰ and 32.1‰, respectively) were larger than expected for heterotrophic metabolisms (Londry et al., 2004).

The $\Delta^{14}C_{PLFA}$ value from BE326 Bh2 was very negative (−941‰), and only slightly enriched in ^{14}C relative to the $\Delta^{14}C_{DIC}$ (−982‰) and $\Delta^{14}C_{CH4}$ (−974‰), and thus was unable to differentiate the microbial carbon sources further than was possible with the $\delta^{13}C$ results (Fig. 3). Notably, replicate $\Delta^{14}C_{DIC}$ and $\Delta^{14}C_{PLFA}$ measurements that were sampled from BE326 Bh2 the following year were shifted towards slightly more positive values ($\Delta^{14}C_{PLFA} = -887‰$ and $\Delta^{14}C_{DIC} = -923‰$), but continued to hold the same offset. Consistent with this observation, the relationship between $\delta^{13}C_{DIC}$ and $\delta^{13}C_{PLFA}$ also remained unchanged over the course of the year ($\Delta\delta^{13}C_{DIC\text{-}PLFA} = 13.9‰$ to 22.7‰ in 2011 and 13.2‰ to 21.6‰ in 2012).

4.3.2. DIC/DOC Cycling Dominant in Deep (>3 km) Microbial Communities

In the two deeper systems (TT107 and TT109 Bh2), isotopic evidence indicated that, despite the presence of high concentrations of CH_4, the microbial ecosystems were primarily utilizing DIC and/or DOC carbon sources. In the case of TT107 (3.1 kmbls), the $\delta^{13}C_{PLFA}$ values were depleted in ^{13}C in relation to DIC, with negative offsets (Fig. 2; $\Delta\delta^{13}C_{DIC\text{-}PLFA} = 6.0‰$ to 20.5‰) that are consistent with the preferential uptake of the lighter isotope of carbon from DIC by the microbial communities (Boschker and Middelburg, 2002; Londry et al., 2004). Concurrently, the PLFAs were enriched in ^{13}C with respect to CH_4, which would be unexpected for methanotrophy (Jahnke et al., 1999; Whiticar, 1999; Valentine and Reeburgh, 2000). Although CH_4 concentrations exceed those of DIC, as was observed in the BE326 boreholes, the $\delta^{13}C_{DIC}$ values do not reflect any input of isotopically depleted carbon derived from microbial methanotrophy. The $\delta^{13}C_{PLFA}$ was enriched in ^{13}C with respect to the DOC values by values ($\Delta^{13}C_{DOC\text{-}PLFA} = -2.7‰$ to −17.2‰; Fig. 2) that overlap the value reported by Londry et al. (2004) for *Desulfotomaculum acetoxidans* grown on acetate ($\Delta^{13}C_{PLFA\text{-}DOC} = 9.5‰$).

The $\Delta^{14}C_{PLFA}$ from TT107 (−633 ± 11‰) was the most enriched of any sample, and supported microbial utilization of DIC (−497 ± 2‰) as a major carbon source (Fig. 3). The difference between $\Delta^{14}C_{DIC}$ and $\Delta^{14}C_{PLFA}$ of 120‰ may indicate that an alternative carbon source with relatively low levels of ^{14}C is being utilized, such as the DOC pool or the abiogenic hydrocarbons, $C_{2\text{-}3}$. An alternative explanation, however, would be that the low concentration of ^{14}C in the PLFAs is due to slow steady-state PLFA biomass turnover rate of 2×10^{-11} yr^{-1} (substituting [$^{14}C_{PLFA}$] for [$^{14}CH_4$] in Eq. (8)). This is equivalent to ~18 cells L^{-1} yr^{-1} or a turnover time based upon the PLFAs of 11,000 years. Such an estimate greatly exceeds the ~1 year cell turnover times derived from amino acid analyses of ~3 km-deep *Firmicutes*-dominated boreholes of slightly greater temperature by Onstott et al. (2014).

The PLFA profile from TT107 mainly consisted of branched PLFAs, which are indicative of Gram-positive bacteria or *Firmicutes* (Fig. 5), which is consistent with the phylogenetic composition of the community as inferred from its metagenome (Magnabosco et al., 2015). The dominance of the acetyl-CoA genes in the metagenomic reads compared to the other carbon fixation pathways (Table 4) and the dominance of *Firmicutes* in the metagenomic data, when combined with the geochemical data, suggest that non-acetogenic, sulphate-reducing bacteria are the primary producers in this fracture water (Magnabosco et al., 2015). Notably, the metagenome sequence data for TT107 detected the highest percentage of genes for methanogenesis. The *in situ* rate of autotrophic methanogenesis of 8.7 ± 2.3 nM/yr is also the highest (Table 2) but, given the young 1 to 6 kyr age of the water, this rate would only produce 12 to 50 μM of CH_4, which is <1% of the observed CH_4 concentration. Although the methanogens are active in this fracture, the subsurface residence time of the water is so brief that insufficient biogenic CH_4 has been produced to significantly influence the observed isotopic signature of the CH_4.

For TT109 Bh2 (3.1 kmbls), the $\Delta^{14}C$ values of the PLFAs (−850‰) and DIC (−863‰) agreed within error (Fig. 3) suggesting that the DIC is the predominant carbon source. The $\delta^{13}C_{PLFA}$ values were depleted in ^{13}C in relation to DIC with negative offsets ($\Delta\delta^{13}C_{PLFA\text{-}DIC} = -21‰$ to −27‰) that are consistent with the preferential uptake of the lighter isotope of carbon from DIC by the microbial communities (Fig. 2). These values are also consistent the those reported for SRB's utilizing the acetyl-CoA pathway and reverse TCA cycle (Londry et al., 2004). PLFAs are generally 3–6‰ more depleted than the bulk microbial biomass; therefore, the $\delta^{13}C$ value of the bulk microbial biomass in TT109 Bh2 could be depleted in ^{13}C by −15‰ to −24‰. This overlaps with the isotopic fractionations expected for microbial utilization of the reductive pentose phosphate cycle (−20‰ to −30‰) and those reported for acetyl-CoA-utilizing methanogens and acetogens (−4‰ to −27‰). However, the isotopic fractionation observed is much greater than the −0.2 to −3.8‰ reported for the 3-HP/4-HB cycle (House et al., 2003; Berg et al., 2010) that is utilized by aerobic Crenarchaeota.

The $\delta^{13}C_{PLFA}$ values from TT109 Bh2 were enriched in ^{13}C in relation to CH_4, which is inconsistent with kinetic isotope effects associated with methanotrophy (Jahnke et al., 1999; Whiticar, 1999; Valentine and Reeburgh, 2000) and the differences in their $\Delta^{14}C$ also precludes the CH_4 from being a significant contributor. The $\delta^{13}C_{PLFA}$ values do directly overlap with the measured $\delta^{13}C_{DOC}$ value (−33.1‰) and may indicate that extracellular organic carbon compounds produced by microorganisms (e.g., excreted polypeptides or polysaccharides) contributed to the DOC in TT109 Bh2 (Fig. 2), as only 3% of the DOC is comprised of formate and acetate (Table 1).

The genetic results indicate that the CO_2 fixation pathways are dominated by the 3-HP/4-HB pathway > the acetyl-CoA pathway > the reductive pentose cycle, or Calvin cycle (Table 4). The limited observation of genes for the Calvin-Benson cycle in this data set may be related to

the paucity of aerobic chemolithoautotrophs that use this pathway, evidenced in the 16S rDNA amplicon datasets (Magnabosco et al. 2014). The abundance of the 3-HP/4-HB pathway is surprising given the paucity of Crenarchaeota in the metagenome and the observed $\Delta\delta^{13}C_{PLFA\text{-}DIC}$ values. The 16S rRNA amplicon data set did reveal the highest relative abundance of aerobic methanotrophs in TT109 Bh2 compared to the other sites, but the lowest relative abundance of methanogens and ANMEs. The *in situ* rates (Table 2) indicate that this less abundant methanogenic population is active and contributing to the overall CH_4 pool. However, the extent of this methanogenic activity and of any methanotrophy that may be utilizing the CH_4 in this system cannot be well constrained, except to say that it has not left a recognizable isotopic or geochemical fingerprint. Overall, the offsets in the $\delta^{13}C$ of the PLFAs with respect to the DIC suggest that the bacteria utilizing the acetyl-CoA pathway are the most active.

4.3.3. A small methanotrophic and methanogenic fraction of the shallow subsurface community plays a large metabolic role

The metagenomic and geochemical datasets indicated that, despite the evidence of CH_4 cycling playing a key role in supporting the microbial communities in the shallower systems, they comprised a small component of the current microbial community. In DR5IPC, the 16S rRNA gene amplicon data (Table 3) indicated that type I and type II methanotrophs accounted for 1% of the bacterial community. At this abundance, their PLFA biomarkers would have been below detection and, indeed, they were not detected. Anaerobic oxidation of CH_4 by a consortium of sulphate-reducing *Deltaproteobacteria* and the ANME group of archaea (Hinrichs et al., 1999; Boetius et al., 2000) could be occurring, but the 16S rRNA gene amplicon data set suggest that the ANME group is at extremely low abundance (Table 3). Although the low concentration of 10Me16:0 precluded the $\delta^{13}C$ analysis of this particular PLFA, its presence at a site where $\delta^{13}C_{PLFA}$ values are −70‰ to −73‰ is consistent with it being derived from CH_4 indirectly via sulphate-reducing bacteria involved in CH_4 cycling. Kotelnikova (2002) also reported anaerobic oxidation of CH_4, coupling to reduction of Fe^{3+}, in enrichments of groundwater samples from the nearby Driefontein shaft #4 borehole into the dolomite aquifer.

In BE326 Bh2, the 16S rRNA gene amplicon data set revealed that 0.3% of the reads were methanogens, 0.1–0.2% were ANME and 1.5–2% were methanotrophs, suggesting that, similar to DR5IPC, the communities sampled at this site also have the potential to cycle CH_4 (Table 3). The most abundant CO_2 fixation genes were those of reductive acetyl-CoA pathway (0.219–0.245%), followed by the reductive pentose pathway (0.072–0.100%) and the 3-HP/4-HB pathway (0.063–0.088%) (Table 4). As noted, while the presence of specific methanotroph biomarker PLFAs could not be confirmed because PLFA double bond positions were not determined, the presence and isotopically depleted nature of 16:1 and 18:1 PLFAs was consistent with the presence of methanotrophs in this system (Fig. 3). These results contrast those reported from 150 to 200 meter deep granite near the Tono uranium mine in Japan where evidence of methanotrophy was identified. In the latter case, the PLFA biomarkers for methanotrophs comprised 3–18% of the PLFAs only and these biomarkers possessed $\delta^{13}C$ values of −60‰ and −93‰, compared to the −95‰ $\delta^{13}C$ value of CH_4 (Mills et al., 2010). The rest of the PLFAs possessed $\delta^{13}C$ values ranging from −28‰ to −45‰.

4.3.3.1. Estimates of CH_4 cycling rates and biomass yields.

Assuming that the 1.5 nM of CH_4 yr^{-1} steady state estimate of the *in situ* microbial CH_4 production rate for Dr5IPC is correct, and assuming 1 mol of ATP is produced per 1 mol of CH_4, and 0.5 g of cellular material is produced per 1 mol of ATP in autotrophic assimilation of CO_2 (lower than experimentally observed yields at high pH; Thauer et al., 2008), then this rate would correspond to 0.75 ng of methanogens yr^{-1}. Assuming that the per cellular mass ranged from 40 to 100 fg, this biosynthesis rate would be equivalent 7500 to 18,800 autotrophic methanogen cells L^{-1} yr^{-1}. If methanogens comprised 1–10% of the total microbial community, then there would be 10^4 to 10^5 methanogens L^{-1}. This would correspond to an autotrophic methanogen turnover time of 1–13 years. The ^{14}C-estimated rate would correspond to a rate of methanogenesis of $1.5 \times 10^{-}$ to 1.5×10^{-14} mol of CH_4 $cell^{-1}$ yr^{-1}, which is faster than the 6.2×10^{-15} mol of CH_4/cell-yr measured by Colwell et al. (2008) for an autotrophic methanogen in a retentostat experiment at 21 °C. The small methanogenic population, in light of such a high *in situ* rate of autotrophic methanogenesis, suggests that an environmental parameter is limiting the population size of the methanogens, such as geochemical conditions resulting in even lower yields, spatially limited anoxic conditions or the lack of critical trace metals.

Oxidation of CH_4 as a carbon source in DR5IPC requires sustained delivery of electron acceptors from the unconfined portion of the dolomite aquifer to the north. In the recharge region, the O_2 concentrations would be close to saturation at 310 μM and the sulphate concentrations are 1000 μM (Onstott et al. 2006). The high sulphate concentrations are due to sulphide oxidation which contributes to the development of karst in the upper ~100 m of the aquifer (Onstott et al., 2006). These values are largely depleted by the time the groundwater reaches the DR5IPC borehole and, dividing by the groundwater age, the combined electron acceptor flux is 80 nM/yr, which is far greater than the estimated methanogenesis rate.

In the case of aerobic methanotrophy, ~8–16 g of cellular material is generated per mole of CH_4 oxidized (Leak and Dalton, 1986a,b). The estimated methanogenesis rate would sustain the production of 12–24 ng of bacterial biomass L^{-1} yr^{-1}, which is equivalent to 1.2 to 6×10^5 cells L^{-1} yr^{-1} or 16–30 times the methanogenic biomass. This biosynthesis rate would also be equivalent to a bacterial cell turnover times of 17–83 years. These turnover times

are consistent with the ~89 year turnover time determined by amino acid racemization analyses of cellular proteins from another planktonic sample from the same dolomite aquifer collected 2 km further west (Onstott et al., 2014). The paucity of aerobic methanotrophs in the microbial community of Dr5IPC (Table 3), therefore, is surprising.

The relative difference in the growth yields between autotrophic methanogens versus bacteria living off energy-rich CH_4 could, in part, explain the relatively higher proportions of bacteria within the current microbial community, but some form of interspecies transfer of isotopically depleted carbon substrates is required. Another potential explanation would be a temporal shift within the system. The observed biogenic CH_4 may have been produced by a community dominated by methanogens that was subsequently out-competed by methanotrophs that are capable of obtaining more energy and/or are not limited by the same parameters as the methanogenic organisms. These methanotrophs may then be providing a more abundant carbon source for heterotrophic organisms that retain the geochemical signatures of the original CH_4 carbon source. In such a system, it may be hypothesized that, over time, key parameters such as the concentration of CH_4 and/or electron acceptors would become depleted and allow the system to cycle back to one dominated by autotrophy rather than heterotrophy. The problem with this ad hoc explanation is that the cause for such cycling is unknown, and microbial communities dominated by Archaea, let alone methanogens, have never been reported in hundreds of sites that have been sampled in the Witwatersrand Basin for the past 15 years.

5. CONCLUSIONS

These results demonstrate that the deep continental subsurface is a highly variable complex system where distinct microbial metabolic activities may support the overall microbial communities. Geochemical evidence of CH_4 cycling was strongest in DR5IPC, but was also resolvable in BE326 Bh1 and Bh2. Despite the fact that the geochemical signal was being driven by CH_4 cycling, DNA evidence for the presence of methanogenic and methanotrophic metabolisms indicated that they comprised a minor component of the current overall microbial community. The capability of a small component of the community to support a much larger community may be related to differences in the relative biomass yields for a given metabolic process and/or temporal variations in conditions potentially alternating between favouring autotrophic versus heterotrophic processes. In the deeper systems, evidence of methanogenic inputs was being swamped by mixing with predominantly abiogenic CH_4 within the system. And despite the presence of high CH_4 concentrations, little evidence of microbial uptake of this CH_4 was detected. Rather, use of DIC and/or DOC was supported. This may be related to the fact that these depths show evidence of mixing of relatively young, meteoric waters being conducted along a dyke with more isolated waters contributing abiogenically-derived CH_4. While such recent mixing might be expected to create an opportunity for extensive microbial utilization of the abundant abiogenic CH_4, it may be that the microbial community is not yet adapted to utilizing this CH_4 as a carbon source. Regardless, these results demonstrate the wide range of potential carbon sources and metabolic pathways that may be active, and may be creating biosignatures, within the deep continental subsurface.

ACKNOWLEDGEMENTS

This work was supported by National Science Foundation (NSF) funding to T.C.O. (EAR-0948659) and T.L.K. (EAR-0948335 and EAR-1141435) and funding from the Natural Science and Engineering Research Council (NSERC) of Canada to G.F.S. via Discovery (RGPIN-288309-2009) and CREATE grants (Canadian Astrobiology Training Program CREAT 371308-09). Metagenome sequencing and analyses of BE2011, BE2012, DR5IPC, T109 Bh2 and TT107 were supported by NASA EPSCoR/New Mexico Space Grant Consortium funding to T.L.K. Metagenome data from sample TT107 were made possible by the Deep Carbon Observatory's Census of Deep Life supported by the Alfred P. Sloan Foundation and partial salary support for several co-authors was from the Deep Carbon Observatory Deep Energy Directorate. Sequencing was performed at the Marine Biological Laboratory (MBL, Woods Hole, MA, USA) and we are grateful for the assistance of Mitch Sogin, Susan Huse, Joseph Vineis, Andrew Voorhis, Sharon Grim, and Hilary Morrison of MBL. C. Magnabosco was supported by the NSF Graduate Research Fellowship to C. Magnabosco (Grant No. DGE-1148900) and the Center for Dark Energy Biosphere Investigations (C-DEBI) Graduate Research Fellowship. (Disclaimer: Any opinion, findings, and conclusions or recommendations expressed in this material are those of the authors and do not necessarily reflect the views of the National Science Foundation. This is C-DEBI contribution 278). We are grateful for the support of Sibanye Gold Ltd. and AngloGold Ashanti Ltd., South Africa and the management and staff of Beatrix, Driefontein, Kloof and Tau Tona mines. We give credits to S. Maphanga of Beatrix Au mine, H. van Niekerk of Driefontein Au mine, and F. Vermeulen, M. Pienaar and A. Munro of Tau Tona Au mine. We thank E. Cason, B. Pfeiffer, C. Simon, Melody Lindsay, L. Snyder, J.-G. Vermeulen, A.M. Meyer, M. Maleke, T. Tlalajoe, V. Mescheryakov, for their assistance in the collection, preservation and field analyses the fracture water samples. We also thank George Rose (Princeton University) who designed and constructed the sampling manifold. Finally we thank Kathryn Elder and Sue Handwork of the NOSAMS facility for processing our ^{14}C samples.

APPENDIX A. SUPPLEMENTARY DATA

Supplementary data associated with this article can be found, in the online version, at http://dx.doi.org/10.1016/j.gca.2015.10.003.

REFERENCES

Apps J. A. and Van de Kamp P. C. (1993) Energy gases of abiogenic origin in the Earth's crust. The future of energy gases. *U.S. Geol. Surv. Prof. Pap.* **1570**, 81–132.

Bau M., Romer R. L., Luders V. and Beukes N. J. (1999) Pb, O and C isotopes in silicified Mooidraai dolomite (Transvaal Supergroup, South Africa): Implications for the composition of the Paleoproterozoic seawater and 'dating' the increase of

oxygen in the Precambrian atmosphere. *Earth Planet. Sci. Lett.* **174**, 43–57.

Beal E. J., House C. H. and Orphan V. J. (2009) Manganese- and iron-dependent marine methane oxidation. *Science* **325**, 184–187.

Berg I. A., Kockelkorn D., Ramos-Vera W. H., Say R. F., Zarzycki J., Hügler M., Alber B. E. and Fuchs G. (2010) Autotrophic carbon fixation in archaea. *Nat. Microbiol. Rev.* **8**, 447–460.

Blaser M. B., Dreisbach L. K. and Conrad R. (2013) Carbon isotope fractionation of 11 acetogenic strains grown on H_2 and CO_2. *Appl. Environ. Microbiol.* **79**, 1787–1794.

Bligh E. G. and Dyer W. J. (1959) A rapid method of total lipid extraction and purification. *Can. J. Biochem. Physiol.* **37**, 911–928.

Bodelier P. L. E., Gillisen M. J. B., Hordijk K., Damste J. S. S., Rijpstra W. I. C., Geenevasen J. A. J. and Dunfield P. F. (2009) A reanalysis of phospholipid fatty acids as ecological biomarkers for methanotrophic bacteria. *ISME J.* **3**, 606–617.

Boetius A., Ravenschlag K., Schubert C. J., Rickert D., Widdel F., Gieseke A., Amann R., Jorgensen B. B., Witte U. and Pfannkuche O. (2000) A marine microbial consortium apparently mediating anaerobic oxidation of methane. *Nature* **407**, 623–626.

Borgonie G., García-Moyano A., Litthauer D., Bert W., Bester A., van Heerden E. and Onstott T. C. (2011) Nematoda from the terrestrial deep subsurface of South Africa. *Nature* **474**, 79–82.

Boschker H. T. S. and Middelburg J. J. (2002) Stable isotopes and biomarkers in microbial ecology. *FEMS Microbiol. Ecol.* **40**, 85–95.

Bowman J. P., Jiménez L., Rosario I., Hazen T. C. and Sayler G. S. (1993) Characterization of the methanotrophic bacterial community present in a trichloroethylene-contaminated subsurface groundwater site. *Appl. Environ. Microbiol.* **59**, 2380–2387.

Bowman J. P. (2006) The methanotrophs: the families methylococcaceae and methylocystaceae. *Prokaryotes* **5**, 266–289.

Brady A. L., Slater G., Laval B. and Lim D. S. (2009) Constraining carbon sources and growth rates of freshwater microbialites in Pavilion Lake using ^{14}C analysis. *Geobiology* **7**, 544–555.

Bredenkamp D. B. and Vogel J. C. (1970) Study of a dolomitic aquifer with carbon-14 and tritium. *Isot. Hydrol.* **1970**, 349–372.

Chivian D., Alm E. J., Brodie E. L., Culley D. E., Dehal P. S., DeSantis Todd. Z., Gihring T. M., Lapidus A., Lin L.-H., Lowry S. R., Moser D. P., Richardson P., Southam G., Wanger G., Pratt L. M., Andersen G. L., Hazen T. C., Brockman F. J., Arkin A. P. and Onstott T. C. (2008) Environmental genomics reveals a single species ecosystem deep within the Earth. *Science* **322**, 275–278.

Clark I. and Fritz P. (1997) *Environmental isotopes in hydrogeology*. CRC Press LLC, Boca Raton, FL, p328.

Coleman M. L., Shepherd T. J., Durham J. J., Rouse J. E. and Moore G. R. (1982) Reduction of water with zinc for hydrogen isotope analysis. *Anal. Chem.* **54**, 993–995.

Colwell F. S., Boyd S., Delwiche M. E., Reed D. W., Phelps T. J. and Newby D. T. (2008) Estimates of biogenic methane production rates in deep marine sediments at hydrate ridge, Cascadia margin. *Appl. Environ. Microbiol.* **74**, 3444–3452.

Epstein S. and Mayeda T. K. (1953) Variations of the $^{18}O/^{16}O$ ratio in natural waters. *Geochim. Cosmochim. Acta* **4**, 213.

Etiope G. and Sherwood Lollar B. (2013) Abiotic methane on Earth. *Rev. Geophys.* **51**, 276–299.

Ettwig K., Butler M., Le Paslier D., Pelletier E., Mangenot S., Kuypers M. M. M., Schreiber F., Dutilh B. E., Zedelius J., de Beer D., Gloerich J., Wessels H. J. C. T., van Alen T., Luesken F., Wu M. L., van de Pas-Schoonen K. T., Op den Camp H. J. M., Janssen-Megens E. M., Francoijs K.-J., Stunnenberg H., Weissenbach J., Jetten M. S. M. and Strous M. (2010) Nitrite-driven anaerobic methane oxidation by oxygenic bacteria. *Nature* **464**, 543–548.

Ettwig K., Speth D. R., Reimann J., Wu M. L., Jetten M. S. M. and Keltjens J. T. (2012) Bacterial oxygen production in the dark. *Front. Microbiol.* **3**, 1–8.

Fang J. S. and Barcelona M. J. (1998) Biogeochemical evidence for microbial community change in a jet fuel hydrocarbons-contaminated aquifer. *Org. Geochem.* **29**, 899–907.

Fritz P., Frape S. K., Drimmie R. J. and Heemskerk A. R. (1986) Reply to comments by Grabczak et al. on Water–rock interaction and chemistry of groundwaters from the Canadian Shield. *Geochim. Cosmochim. Acta* **50**, 1561–1563.

Gebert J., Grongroft A., Schloter M. and Gattinger A. (2004) Community structure in a methanotroph by phospholipid fatty acid biofilter as revealed analysis. *FEMS Microbiol. Lett.* **240**, 61–68.

Green C. T. and Scow K. M. (2000) Analysis of phospholipid fatty acids (PLFA) to characterize microbial communities in aquifers. *Hydrogeol. J.* **8**, 126–141.

Guckert J. B., Antworth C. P., Nichols P. D. and White D. C. (1985) Phospholipid, ester-linked fatty-acid profiles as reproducible assays for changes in prokaryotic community structure of estuarine sediments. *FEMS Microbiol. Ecol.* **31**, 147–158.

Guckert J. B., Hood M. A. and White D. C. (1986) Phospholipid ester-linked fatty-acid profile changes during nutrient deprivation of vibrio-cholerae – increases in the trans cis ratio and proportions of cyclopropyl fatty-acids. *Appl. Environ. Microbiol.* **52**, 794–801.

Hardwood D. L. and Russell N. J. (1984) *Lipids in plants and microbes*. George Allen and Unwin, London.

Haroon M. F., Hu S., Shi Y., Imelfort M., Keller J., Hugenholtz P., Yuan Z. and Tyson G. W. (2013) Anaerobic oxidation of methane coupled to nitrate reduction in a novel archaeal lineage. *Nature* **500**, 567–570.

Hayes J. M. (2001) Fractionation of carbon and hydrogen isotopes in biosynthetic processes. *Stable Isot. Geochem.* **43**, 225–277.

Heesakkers V., Murphy S., Lockner D. A. and Reches Z. (2011) Earthquake rupture at focal depth, part II: mechanics of the 2004 M2.2 earthquake along the pretorius fault, Tautona mine, South Africa. *Pure Appl. Geophys.* **168**, 2427–2449.

Hinrichs K. U., Hayes J. M., Sylva S. P., Brewer P. G. and DeLong E. F. (1999) Methane-consuming archaebacteria in marine sediments. *Nature* **398**, 802–805.

Hoehler T. M., Alperin M. J., Albert D. B. and Martens C. S. (1994) Field and laboratory studies of methane oxidation in an anoxic marine sediment – evidence for a methanogen-sulfate reducer consortium. *Global Biogeochem. Cycles* **8**, 451–463.

House C. H., Schopf J. W. and Stetter K. O. (2003) Carbon isotopic fractionation by Archaeans and other thermophilic prokaryotes. *Org. Geochem.* **34**, 345–356.

Hügler M. and Sievert S. M. (2011) Beyond the Calvin cycle: autotrophic carbon fixation in the ocean. *Annu. Rev. Marine Sci.* **3**, 261–289.

Hunt J. M. (1996) *Petroleum geochemistry and geology*. W. H. Freeman and Company, New York, 743 pp.

Jahnke L. L., Summons R. E., Hope J. M. and des Marais D. J. (1999) Carbon isotopic fractionation in lipids from methanotrophic bacteria II: the effects of physiology and environmental parameters on the biosynthesis and isotopic signatures of biomarkers. *Geochim. Cosmochim. Acta* **63**, 79–93.

Kaneda T. (1991) Iso-fatty and anteiso-fatty acids in bacteria – biosynthesis, function, and taxonomic significance. *Microbiol. Rev.* **55**, 288–302.

Kieft T. L., Ringelberg D. B. and White D. C. (1994) Changes in ester-linked phospholipid fatty- acid profiles of subsurface bacteria during starvation and dessication in a porous medium. *Appl. Environ. Microbiol.* **60**, 3292–3299.

Knittel K. and Boetius A. (2009) Anaerobic oxidation of methane: progress with an unknown process. *Annu. Rev. Microbiol.* **63**, 311–334.

Kotelnikova S. (2002) Microbial production and oxidation of methane in deep subsurface. *Earth Sci. Rev.* **58**, 367–395.

Lau M. C. Y., Cameron C., Magnabosco C., Brown C. T., Schilkey F., Grim S., Hendrickson S., Pullin M., Sherwood Lollar B., Esta van Heerden, Kieft T. L. and Onstott T. C. (2014) Phylogeny and phylogeography of functional genes shared among seven terrestrial subsurface metagenomes reveal N-cycling and microbial evolutionary relationships. *Front. Microbiol.* **5**, 531.

Leak D. and Dalton H. (1986a) Growth yields of methanotrophs 1. *Appl. Microbiol. Biotechnol.* **23**, 470–476.

Leak D. and Dalton H. (1986b) Growth yields of methanotrophs 2: a theoretical analysis. *Appl. Microbiol. Biotechnol.* **23**, 477–481.

Lin L. H., Hall J., Lippmann-Pipke J., Ward J. A., Sherwood Lollar B., DeFlaun M., Rothmel R., Moser D., Gihring T. M., Mislowack B. and Onstott T. C. (2005) Radiolytic H_2 in continental crust: nuclear power for deep subsurface microbial communities. *Geochem. Geophys. Geosyst.* **6**, 13.

Lin L.-H., Gihring T. M., Sherwood Lollar B., Boice E., Pratt L. M., Lippmann-Pipke J., Bellamy R. E. S., Hall J. and Onstott T. C. (2006) Planktonic microbial communities associated with fracture-derived groundwater in a deep gold mine of South Africa. *Geomicrobiol. J.* **23**, 474–497.

Londry K. L., Jahnke L. L. and Marais D. J. D. (2004) Stable carbon isotope ratios of lipid biomarkers of sulfate-reducing bacteria. *Appl. Environ. Microbiol.* **70**, 745–751.

Londry K. L., Dawson K. G., Grover H. D., Summons R. E. and Bradley A. S. (2008) Stable carbon isotope fractionation between substrates and products of *Methanosarcina barkeri*. *Org. Geochem.* **39**, 608–621.

Magnabosco C., Tekere M., Lau M. C. Y., Linage B., Kuloyo O., Erasmus M., Cason E., van Heerdeen E., Borgonie G., Kieft T. L., Olivier J. and Onstott T. C. (2014) Comparisons of the composition and biogeographic distribution of the bacterial communities occupying South African hot springs with those inhabiting the deep subsurface fracture water. *Front. Microbiol.* http://dx.doi.org/10.3389/fmicb.2014.00679.

Magnabosco C., Ryan K., Lau M. C. Y., Kuloyo O., Sherwood Lollar B., Kieft T. L., van Heerden E. and Onstott T. C. (2015) A metagenomic window into carbon metabolism at 3 km depth in Precambrian continental crust. ISME J., 1–12.

Mailloux B. J., Dochenetz A., Bishop M., Dong H., Ziolkowski L. A., Wommack K. E., Sakowski E. G., Onstott T. C. and Slater G. F. (2012) A carbon free filter for collection of large volume samples of cellular biomass from oligotrophic waters. *J. Microbiol. Methods* **90**, 145–151.

Manzi M. S. D., Durrheim R. J., Hein K. A. A. and King N. (2012) 3D edge detection seismic attributes used to map potential conduits for water and methane in deep gold mines in the Witwatersrand basin, South Africa. *Geophysics* **77**, 133–147.

McNichol A. P., Osborne E. A., Gagnon A. R., Fry B. and Jones G. A. (1994) TIC, TOC, DIC, DOC, PIC, POC – unique aspects in the preparation of oceanographic samples for C-14 AMS. *Nucl. Instrum. Methods Phys. Res., Sect. B* **92**, 162–165.

Meyer F., Paarmann D. M. D. S., Olson R., Glass E. M. and Kubal M. (2008) The metagenomics RAST server – a public resource for the automatic phylogenetic and functional analysis of metagenomes. *BMC Bioinformatics* **9**, 386.

Mills C. T., Amano Y., Slater G. F., Dias R. F., Iwatsuki T. and Mandernack K. W. (2010) Microbial carbon cycling in oligotrophic regional aquifers near the Tono Uranium Mine, Japan as inferred from delta C-13 and Delta C-14 values of *in situ* phospholipid fatty acids and carbon sources. *Geochim. Cosmochim. Acta* **74**, 3785–3805.

Mills C. T., Slater G. F., Dias R. F., Carr S. A., Reddy C. M., Schmidt R. and Mandernack K. W. (2013) The relative contribution of methanotrophs to microbial communities and carbon cycling in soil overlying a coal-bed methane seep. *FEMS Microbiol. Ecol.* **84**, 474–494.

Milucka J., Ferdelman T. G., Polerecky L., Franzke D., Wegener G., Schmid M., Lieberwirth I., Wagner M., Widdel F. and Kuypers M. M. M. (2012) Zero-valent sulphur is a key intermediate in marine methane oxidation. *Nature* **491**, 541.

Onstott T. C., Phelps T. J., Colwell F. S., Ringelberg D., White D. C., Boone D. R., McKinley J. P., Stevens T. O., Long P. E., Balkwill D. L., Griffin W. T. and Kieft T. (1998) Observations pertaining to the origin and ecology of microorganisms recovered from the deep subsurface of Taylorsville Basin, Virginia. *Geomicrobiol. J.* **15**, 353–385.

Onstott T. C., Lin L. H., Davidson M., Mislowack B., Borcsik M., Hall J., Slater G., Ward J., Sherwood Lollar B., Lippmann-Pipke J., Boice E., Pratt L. M., Pfiffner S., Moser D., Gihring T., Kieft T. L., Phelps T. J., Vanheerden E., Litthaur D., Deflaun M., Rothmel R., Wanger G. and Southam G. (2006) The origin and age of biogeochemical trends in deep fracture water of the Witwatersrand Basin, South Africa. *Geomicrobiol. J.* **23**, 369–414.

Onstott T. C., van Heerden E. and Murdoch L. (2010) Microbial life in the depths of the Earth. *Geosciences, la revue du BRGM pour une Terre Durable* **11**, 52–59.

Onstott T. C., Magnabosco C., Aubrey A. D., Burton A. S., Dworkin J. P., Elsila J. E., Grunsfeld S., Cao B. H., Hein J. E., Glavin D. P., Kieft T. L., Silver B. J., vanHeerden E., Opperman D. J. and Bada J. L. (2014) Does aspartic acid racemization constrain the depth limit of the subsurface biosphere? *Geobiology* **12**, 1–19.

Pedersen K. (1997) Microbial life in deep granitic rock. *FEMS Microbiol. Rev.* **20**, 399–414.

Pedersen K. (2000) Exploration of deep intraterrestrial microbial life: current perspectives. *FEMS Microbiol. Lett.* **185**, 9–16.

Petsch S. T., Eglinton T. I. and Edwards K. J. (2001) ^{14}C-Dead living biomass: evidence for microbial assimilation of ancient organic carbon during shale weathering. *Science* **292**, 1127–1131.

Pfiffner S. M., Cantu J. M., Smithgall A., Peacock A. D., White D. C., Moser D. P., Onstott T. C. and van Heerden E. (2006) Deep subsurface microbial biomass and community structure in Witwatersrand Basin mines. *Geomicrobiol. J.* **23**, 431–442.

Porter K. G. and Feig Y. S. (1980) The use of DAPI for identifying and counting aquatic microflora. *Limnol. Oceanogr.* **25**(5), 943–948.

Raghoebarsing A. A., Pol A., van de Pas-Schoonen K. T., Smolders A. J. P., Ettwig K. F., Rijpstra W. I. C., Schouten S., Sinninghe Damste´ J. S., Op den Camp H. J. M., Jetten M. S. M. and Strous M. (2006) A microbial consortium couples anaerobic methane oxidation to denitrification. *Nature* **440**, 918–921.

Ruby E. G., Jannasch H. W. and Deuser W. G. (1987) Fractionation of stable carbon isotopes during chemoautotrophic growth of sulfur-oxidizing bacteria. *Appl. Environ. Microbiol.* **53**, 1940–1943.

Schoell M. (1988) Multiple origins of methane in the Earth. *Chem. Geol.* **71**, 1–10.

Seifert A. G., Trumbore S., Xu X. M., Zhang D. C. and Gleixner G. (2013) Variable effects of plant colonization on black slate update into microbial PLFAs. *Geochim. Cosmochim. Acta* **106**, 391–403.

Sessions A. L. (2006) Isotope-ratio detection for gas chromatography. *J. Sep. Sci.* **29**, 1946–1961.

Silver B. J., Raymond R., Sigman D., Prokopenko M., Sherwood Lollar B., Lacrampe-Couloume G., Fogel M., Pratt L., Lefticariu L. and Onstott T. C. (2012) The origin of NO_3^- and N_2 in deep subsurface fracture water of South Africa. *Chem. Geol.* **294–295**, 51–62.

Sherwood Lollar B., Westgate T. D., Ward J. A., Slater G. F. and Lacrampe-Couloume G. (2002) Abiogenic formation of alkanes in the Earth's crust as a minor source for global hydrocarbon reservoirs. *Nature* **416**, 522–524.

Sherwood Lollar B., Lacrampe-Couloume G., Slater G. F., Ward J., Moser D. P., Gihring T. M., Lin L. H. and Onstott T. C. (2006) Unravelling abiogenic and biogenic sources of methane in the Earth's deep subsurface. *Chem. Geol.* **226**, 328–339.

Slater G. F., White H. K., Eglinton T. I. and Reddy C. M. (2005) Determination of microbial carbon sources in petroleum contaminated sediments using molecular C-14 analysis. *Environ. Sci. Technol.* **39**, 2552–2558.

Slater G. F., Lippmann-Pipke J., Moser D. P., Reddy C. M., Onstott T. C., Lacrampe-Couloume G. and Sherwood Lollar B. (2006) C-14 in methane and DIC in the deep terrestrial subsurface. Implications for microbial methanogenesis. *Geomicrobiol. J.* **23**, 453–462.

Stevens T. O. and McKinley J. P. (1995) Lithoautotrophic microbial ecosystems in deep basalt aquifers. *Science* **270**, 450–454.

Stuiver, M., and H. A. Polach (1977) Discussion – Reporting of 14C data. Radiocarbon, 355–363.

Teece M. A., Fogel M. L., Dollhopf M. E. and Nealson K. H. (1999) Isotopic fractionation associated with biosynthesis of fatty acids by a marine bacterium under oxic and anoxic conditions. *Org. Geochem.* **30**, 1571–1579.

Templeton A. S., Chu K.-H., Alvarez-Cohen L. and Conrad M. E. (2006) Variable carbon isotope fractionation expressed by aerobic CH_4-oxidizing bacteria. *Geochim. Cosmochim. Acta* **70**, 1739–1752.

Thauer R. K., Kaster A.-K., Seedorf H., Buckel W. and Hedderich R. (2008) Methanogenic archaea: ecologically relevant differences in energy conservation. *Nat. Rev. Microbiol.* **6**, 579–591.

Valentine D. L. and Reeburgh W. S. (2000) New perspectives on anaerobic methane oxidation. *Environ. Microbiol.* **2**, 477–484.

Wanger G., Southam G. and Onstott T. C. (2006) Structural and chemical characterization of a natural fracture surface from 2.8 km below land surface. Biofilms in the deep subsurface. *Geomicrobiol. J.* **23**, 443–452.

Ward J. A., Slater G. F., Moser D. P., Lin L. H., Lacrampe-Couloume G., Bonin A. S., Davidson M., Hall J. A., Mislowack B., Bellamy R. E. S., Onstott T. C. and Sherwood Lollar B. (2004) Microbial hydrocarbon gases in the Witwatersrand Basin, South Africa: implications for the deep biosphere. *Geochim. Cosmochim. Acta* **68**, 3239–3250.

Whiticar M. J. (1999) Carbon and hydrogen isotope systematics of bacterial formation and oxidation of methane. *Chem. Geol.* **161**, 291–314.

Whitman W. B., Coleman D. C. and Wiebe W. J. (1998) Prokaryotes: the unseen majority. *Proc. Natl. Acad. Sci.* **95**, 6578–6583.

Associate editor: Tom McCollom